LITHOS 482–483 (2024) 107704

Contents lists available at ScienceDirect

LITHOS

journal homepage: www.elsevier.com/locate/lithos

On the occurrence of kalsilite in melilite-bearing ultrapotassic lavas from the Roman Province (Vulsini Mts., central Italy)

Francesca Innocenzi [a,b,c], Sara Ronca [a,*], Samuele Agostini [b], Federica Benedetti [a], Michele Lustrino [a,d]

[a] Dipartimento di Scienze della Terra, Sapienza Università di Roma, P.le A. Moro, 5, 00185 Roma, Italy
[b] Istituto di Geoscienze e Georisorse – CNR, Via Moruzzi, 1, 56124 Roma, Italy
[c] School of Natural Sciences, Macquarie University, North Ryde, New South Wales 2109, Australia
[d] Istituto di Geologia Ambientale e Geoingegneria – CNR, c/o Dipartimento di Scienze della Terra, Sapienza Università di Roma, P.le A. Moro, 5, 00185 Roma, Italy

ARTICLE INFO

Keywords:
Ultrapotassic magmatism
Roman Province
Kalsilite

ABSTRACT

The Montefiascone Volcanic Complex belongs to the Vulsini Mts. volcanic district, one of the several leucite-bearing ultrapotassic Pleistocene volcanoes of the Roman Province (Central Italy). It is characterized by abundant pyroclastic successions and minor lava flows emplaced during a caldera formation phase occurred ~0.3–0.2 Ma. The volcanic products span from leucite-basanites and leucite-tephrites to rarer leucitites and melilitites, occasionally associated with very rare kalsilite melilitolite ejecta. Here we report for the first time the presence of primary kalsilite in two lava flows in Forcinella and Feltricci localities, identifying a kamafugitic component among the Montefiascone volcanics.

Detailed petrographic, SEM and EPMA studies on ten samples from the two localities revealed, in addition to kalsilite, variable amounts of clinopyroxene, melilite, leucite and nepheline plus rarer olivine coupled with carbonate-bearing segregation pockets in the groundmass. Geochemical and isotopic data confirm the exotic nature of the analysed rocks, showing ultrabasic/basic (SiO_2 = 42.15–45.94 wt%) and ultrapotassic (K_2O = 6.17–8.48 wt%; K_2O/Na_2O = 5.3–8.7) compositions, as well as strongly radiogenic $^{87}Sr/^{86}Sr$ (0.71038–0.711068), poorly radiogenic $^{143}Nd/^{144}Nd$ (0.512057.512091) and uniform middle radiogenic $^{206}Pb/^{204}Pb$ (18.76–18.78). Boron isotopes ($\delta^{11}B$ ranges from 7.36 to 8.82‰) almost overlaps the typical MORB-OIB range values.

These geochemical features recall those of the nearby kamafugite rocks from the Intra-Apennine Province. Major oxide and trace element modelling support fractionation links among the Italian kamafugite types. The overall geochemical and isotopic signatures speak for a common strongly subduction-metasomatized and orthopyroxene-free lithospheric mantle source. As already proposed for some nearby kamafugite centres in central Italy, limestone assimilation during magma ascent is a viable option to explain the mineralogical and whole-rock composition of Montefiascone lavas (i.e., the presence of carbonate plagues in the lava groundmass). This is particularly relevant considering the thick sedimentary sequence pierced by the limited volume of the upwelling magma. On the other hand, many other key features (such as the general lack of crustal xenoliths, the overall incompatible element fractionation and the radiogenic Sr isotopic ratios) clearly require also derivation from subduction-modified mantle sources.

1. Introduction

Kalsilite ($KAlSiO_4$), as part of the nepheline group, is a very rare mineral mostly found in volcanic rocks, with rarer occurrences in plutonic terms (e.g., Bea et al., 2014; Deer et al., 2013). Kalsilite may occur both in strongly SiO_2-undersaturated, strongly ultrabasic (SiO_2 ~ 30–40 wt%) mildly alkaline potassic rocks (e.g., Melluso et al., 2008; Velásquez Ruiz et al., 2022; Innocenzi et al., 2024) or in moderately SiO_2-undersaturated, moderately ultrabasic (SiO_2 ~ 40–48 wt%) strongly ultrapotassic compositions (Lustrino et al., 2020). Kalsilite crystallizes in melts with high K_2O/SiO_2 ratios, with limited constraints on the absolute amounts of K_2O and SiO_2. The presence of primary

* Corresponding author at: Dipartimento di Scienze della Terra, Sapienza Università di Roma, P.le A. Moro, 5, 00185 Roma, Italy.
E-mail address: sara.ronca@uniroma1.it (S. Ronca).

https://doi.org/10.1016/j.lithos.2024.107704
Received 31 January 2024; Received in revised form 12 June 2024; Accepted 20 June 2024
Available online 22 June 2024

kalsilite in igneous rocks is such a distinctive feature that IUGS used this mineral to identify a specific rock group (i.e., kalsilite-bearing volcanic rocks, also known as kamafugites; Le Maitre, 2002).

We emphasize the importance of kalsilite primary origin, considering that $KAlSiO_4$ can be also found as kaliophilite polymorph (e.g., in the potassic and ultrapotassic products of the Somma-Vesuvius and the Roman Volcanic Province; Cellai et al., 1992; Di Battistini et al., 2001; Peccerillo et al., 2010; Lustrino et al., 2020; Mugnaioli et al., 2020) and as perthite-like intergrowths associated to nepheline, due to exsolution from K-rich nepheline (Deer et al., 2013; Franco and De Gennaro, 1988; Sahama, 1962).

To date, kalsilite-bearing volcanic rocks have been reported only in three areas worldwide, i.e., SW Uganda (Toro-Ankole), Central Italy (San Venanzo and Cupaello) and SE Brazil (Alto Paranaíba and Goiás Alkaline Provinces; Stoppa and Cundari, 1996; Brod et al., 2005; Lustrino et al., 2020; Innocenzi et al., 2023, 2024; Velásquez Ruiz et al., 2022). In the present study, we report the first occurrence of kalsilite also in the melilitite-bearing lavas from the Montefiascone volcanic complex (Vulsini Mts.), where it was previously reported in crystalline ejecta only (i.e., kalsilite melilitolite; Di Battistini et al., 2001). A detailed study on Montefiascone kamafugites, also comparing them with the other Italian kalsilite-bearing rocks, may be crucial in achieving a better knowledge of these rare lithologies, as well as their mantle sources and petrogenesis.

1.1. *Worldwide occurrences of the kalsilite-bearing volcanic rocks*

Holmes (1950) was the first to point out the importance of kalsilite in volcanic rocks, identifying three variants in the Toro Ankole lavas (Western branch of the East Africa Rift - WEAR; Innocenzi et al., 2024).

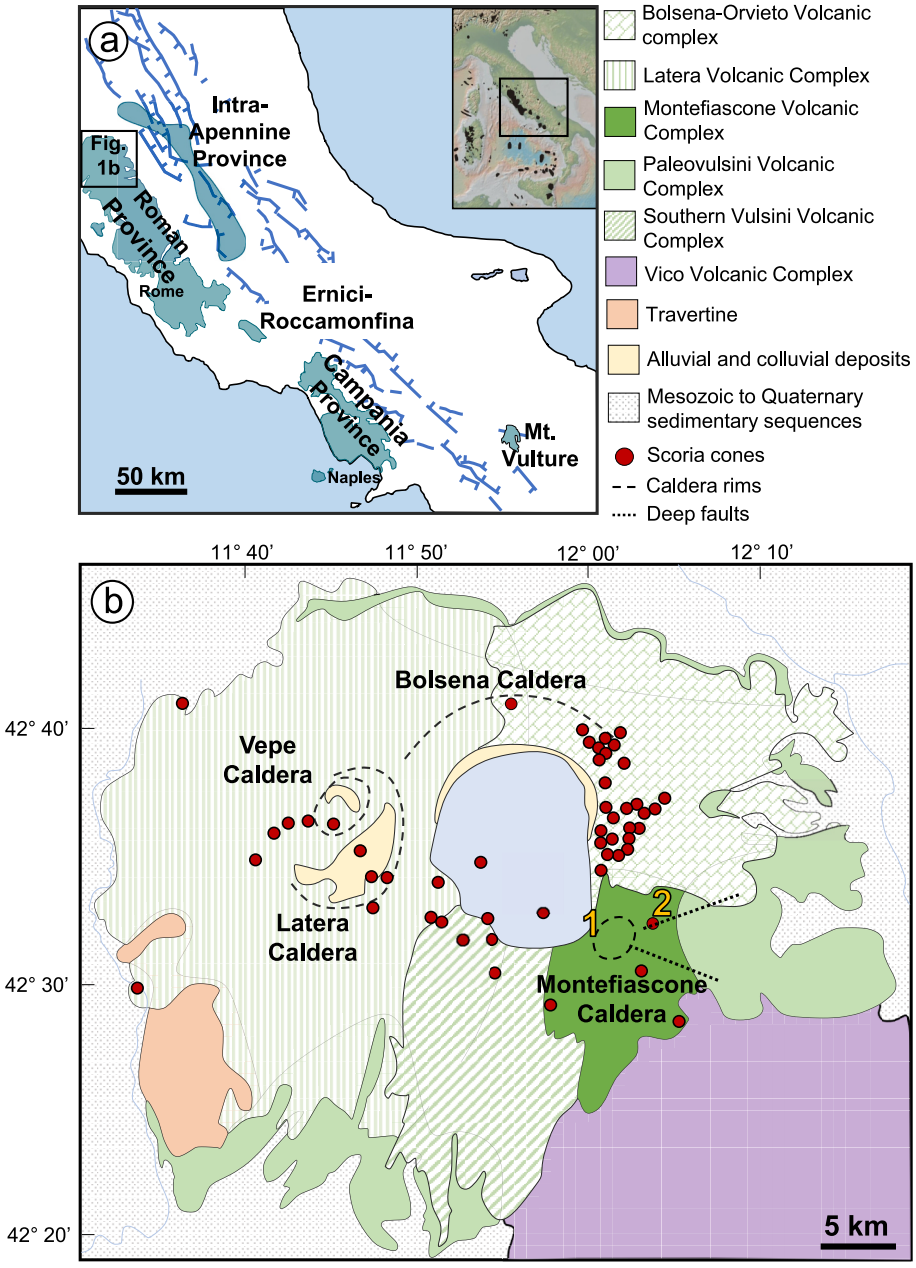

Fig. 1. a) Simplified sketch map of the central Italy area with the main volcanic provinces, from north to south: Intra-Apennine Province (IAP), Roman Province, Ernici-Roccamonfina, Campania Province and the Mt. Vulture volcano. Modified after Lustrino et al. (2020). b) Geological map of the Vulsini Volcanic District showing the main volcanic complexes, caldera structures and emission centres. Modified after Palladino et al. (2010) and Marra et al. (2020). 1 = Forcinella lava; 2 = Feltricci lava. Deep fault structures are from Di Filippo et al. (1999).

These three rock types, named Katungite (kalsilite leucite melilitite), Mafurite (leucite melilite kalsilitite) and Ugandite (melilite kalsilite leucitite), were later grouped under the acronym KaMafUgite (Le Maitre, 2002; Sahama, 1974). Clinopyroxene, olivine and phlogopite are common minerals in all the three variants.

Few decades later, primary kalsilite was also identified in volcanic rocks from the Intra-Apennine Province (IAP, Central Italy; Gallo et al., 1984; Lustrino et al., 2020), in the Alto Paranaíba Igneous Province (APIP; Sgarbi and Valenca, 1993; Velásquez Ruiz et al., 2022) and, more recently, in the Goiás Alkaline Province (GAP; Brazil; Brod et al., 2005).

IAP is a Pleistocene volcanic province consisting of small eruptive vents found along the central Apennine Chain (Melluso et al., 2003; Peccerillo, 2017; Lustrino et al., 2019, 2020; Fig. 1). IAP is relevant in petrology because it comprises the other two terms (venanzite – kalsilite phlogopite olivine leucite melilitite – and coppaelite – kalsilite phlogopite melilitite) belonging to the kalsilite-bearing volcanic rock group identified by IUGS (Le Maitre, 2002; Woolley et al., 1996). IAP products span from strongly ultrabasic to intermediate compositions and from ultrapotassic to nearly alkali-free terms. The whole-rock and modal composition of IAP rocks is variable, not always reflecting primary magmatic compositions. Indeed, in several cases (e.g., Polino, Cupaello and San Venanzo), the assimilation of crustal carbonates during the ascent of SiO_2-poor magmas, has been considered to have strongly modified the composition of the original mantle melts (e.g., Gallo et al., 1984; Lustrino et al., 2019, 2020, 2022b; Peccerillo, 1998, 2017). Further, other IAP products (e.g., Colle Fabbri and Ricetto) have been interpreted as the result of carbonate and marl melting, later solidified as wollastonite- and melilite-bearing paralavas (Melluso et al., 2003).

2. Geological background

The Vulsini Mts. volcanic district (~0.6–0.1 Ma; Nicoletti et al., 1981; Nappi et al., 1995; Marra et al., 2020) is located in the western margin of the Central Apennine (Latium region), in the northernmost part of the Quaternary Roman Province (Fig. 1a; Conticelli et al., 2010; Peccerillo, 2017; Branca et al., 2023), covering an area of ~2200 km^2. The volcanic rocks cover Mesozoic to Neogene sedimentary units, folded and thrust during a mid-late Miocene compressive tectonic phase and later affected by Messinian to Plio-Pleistocene extensional tectonics (Barchi et al., 2001; Nappi et al., 2019). Such extensional phase, related to the Tyrrhenian See opening (Acocella et al., 2012; Acocella and Funiciello, 2006; Peccerillo, 2017), led to the formation of NW-SE-oriented horst and graben structures, later filled by sedimentary deposits of marine to continental environments (Nappi et al., 2019).

The Vulsini Mts. volcanic district includes more than a hundred emission centres (Palladino et al., 2010) grouped into five main volcanic complexes: Bolsena-Orvieto, Latera, Montefiascone, Paleovulsini and Southern Vulsini (Fig. 1b), almost entirely characterized by explosive activities (Strombolian, Plinian, and phreatomagmatic types). This eruptive style, locally associated with small-scale lava flows, is associated to the development of several caldera structures, among which the polygenic Bolsena caldera (~0.6–0.2 Ma; Nappi et al., 1991, 1995; Funiciello et al., 2012) is the largest, with a diameter of ~19 km. The two other most relevant structures are the Latera-Vepe caldera (~0.26–0.16 Ma; Turbeville, 1992; Nappi et al., 1995; Palladino and Simei, 2005; Palladino et al., 2014) and the Montefiascone caldera (~0.29–0.23 Ma; Fig. 1b; Nappi et al., 1995; Brocchini et al., 2000; Palladino and Simei, 2002; Palladino et al., 2010, 2014; Acocella et al., 2012; Peccerillo, 2017).

The Montefiascone polygenetic caldera is ~3 km in diameter, centred on the top of a collapsed central edifice (Marini and Nappi, 1986; Palladino et al., 2010, 2014). The pre-caldera volcanic activity in this area mainly produced leucitite lava flows in the southern part (e.g., Commenda lava), followed by a first ignimbrite eruption (Montefiascone basal ignimbrite; Palladino et al., 2010), corresponding to the main phase of the caldera formation. This stage was succeeded by a first hydromagmatic phase and many other caldera-forming eruptions, leading to new structural collapses (e.g., Marini and Nappi, 1986). The 'lavadrop ignimbrite' was emplaced probably during the second caldera-forming event. Later, two hydromagmatic phases took place (Marini and Nappi, 1986). The hydromagmatic activity produced pyroclastic (such as the Ciuccara products; Nappi et al., 2019) and Strombolian deposits, coupled with small lava flows, in the peri-caldera and circum-caldera areas (Marini and Nappi, 1986; Palladino et al., 2010). The last magmatic phases led to the emplacement of tephrite, basanite and melilitite lava flows (Nappi et al., 2019). The total volume of products estimated for the Montefiascone Volcanic complex is ~10 km^3 (Acocella et al., 2012).

The sedimentary substratum of the Montefiascone caldera, such as the entire Vulsini Mts. district, is characterized by a ~ 5–6 km thick sequence of marls, sandstones and limestones, deposited during Mesozoic, Paleogene and Neogene (e.g., Buonasorte et al., 1987; Di Battistini et al., 2001). In particular, a borehole drilled in the Montefiascone area revealed underneath the Plio-Pleistocene post-collisional sequence, the presence of Ligurian units, mostly consisting of calcareous and marly-calcareous flysch, overlapping the Tuscan series deposits, as biocalcarenite, biocalcirudite, limestone and sandstone (Cretaceous to Oligocene; Buonasorte et al., 1987).

The volcanic products from the Vulsini Mts. district span a large compositional range (Supplementary material 1). Most of the Bolsena-Orvieto, Latera, Paleovulsini and Southern Vulsini volcanic complex products have trachytic, phonotephritic and phonolitic compositions, with Bolsena-Orvieto complex including leucite tephrites, and rarer shoshonites and latites, while Latera products reach trachybasaltic compositions (e.g., Civetta et al., 1984; Conticelli et al., 1987; Peccerillo, 2017; Varekamp and Kalamarides, 1989). All the Vulsini Mts. products belong to the so-called Potassic Series (KS, also known as Saturated Series, from trachybasalts up to trachytes) and to the High Potassium Series (HKS, with compositions ranging from leucitites to phonolites), widely distributed within the entire Roman Comagmatic Region (Peccerillo, 2017). Vulsini Mts. volcanic rocks are enriched in incompatible trace elements and are characterized by strongly radiogenic Sr ratios, coupled with unradiogenic Nd and middle radiogenic Pb compositions (e.g., Civetta et al., 1984; Conticelli et al., 2002; Conticelli and Peccerillo, 1992; Peccerillo, 2017; Rogers et al., 1985).

Montefiascone volcanic rocks mainly consist of leucite basanites, leucite tephrites and leucitites (Coltorti et al., 1991; Di Battistini et al., 1998, 2001; Nappi et al., 1998; Peccerillo, 2017). Kalsilite melilitolite ejecta have been also rarely found (Di Battistini et al., 2001). Small and thin (<3 m thick) melilite-bearing lava flows have been reported in two localities known as Forcinella (cropping out near the south-eastern shore of the Bolsena Lake) and the Feltricci (along the Feltricci stream; Fig. 1b; Di Battistini et al., 2001). Radiometric dating for these two occurrences is still lacking, but stratigraphic and field data indicate that they have been likely emplaced in the 292–227 kyr interval, covering the Montefiascone basal ignimbrite (292 ka) and overlain by the Orto Piatto lava (~227 ka; Di Battistini et al., 2001; Nappi et al., 2019). The Feltricci lava is probably coeval with the Fastello Group rocks (<247 kyr), as reported in the CARG 1:50000 Sheet 345 "Viterbo".

3. Sampling and analytical methods

Ten lava rocks samples have been collected from the two outcrops (sampling sites are reported in Supplementary material 1). Unfortunately, both Feltricci and Forcinella outcrops are not entirely accessible, as they are found along a streamline. In addition, the widespread vegetation cover, coupled with several anthropic structures, prevented the attainment of a detailed macro-scale investigation of the two lava flows. For more details about the field data, we refer to the Viterbo and Tuscania sheets of the 1:50.000 Italian geological map (CARG project).

Polished thin sections for all the ten collected samples from the Forcinella e Feltricci lava flows were prepared in the laboratories of the

Dipartimento di Scienze della Terra of the Sapienza University. Following polarized light microscopy observations on the thin sections, SEM-EDS and EPMA investigations were carried out on the most representative samples. Qualitative mineral chemical and microstructural analyses have been carried out using a Scanning Electron Microscopy (FEI Quanta 400 instrument, with EDAX Genesis microanalysis system and with a 25–30 kV accelerating voltage) at the Dipartimento di Scienze della Terra of Sapienza University. Quantitative chemical analyses on the main mineral phases and glasses were carried out at the Istituto di Geologia Ambientale e Geoingegneria (CNR), Sapienza University, with a CAMECA SX 50 EPMA, with a full wavelength-dispersive mode, a 15 kV accelerating voltage, 15 nA beam current, beam diameter ranging from 1 to 10 μm, 20 s time of counting peak and 10 s time for background. Quantitative chemical analyses on the mineral phases and glass were also carried out at the Macquarie GeoAnalytical Laboratories (MQGA) of Macquarie University (Sydney, Australia) by means of a SEM Zeiss EVO MA15, operating at 20 kV and a working distance of 12 mm. Mineralogical mapping of the samples has been processed with a FEI–-Field Emission Scanning Electron Microscope (MQGA). The instrument works at 15 kV, using a beam current 11 nA, a spot size 15 μm and a working distance 10 mm.

On five of the most representative and unaltered samples, whole-rock major oxide and trace element chemical analyses were performed by inductively coupled plasma-atomic emission spectroscopy (ICP-AES through lithium metaborate/tetraborate fusion) and ICP-mass spectrometry (ICP-MS), at Activation Laboratories Inc. (Ontario, Canada) according to the Code 4Litho code package. The mass loss on ignition (reported as LOI) was determined by standard gravimetric methods and the CO_2 by infrared spectroscopy. Details on the precision and accuracy of the analyses are reported at https://actlabs.com/.

Three representative samples were selected for radiogenic (Sr, Nd, Pb) and stable isotope (B) investigation using a ThermoFisher Neptune Plus MC-ICP-MS, at the Istituto di Geoscienze e Georisorse (IGG-CNR) of Pisa. For radiogenic isotopes, analyses were carried out on powdered whole-rock samples after digestion via concentrated HF + HNO_3 and sample purification through conventional cation-ion exchange chromatography. For B analyses, powdered whole rocks samples were fused in Pt—Ir crucibles after adding K_2CO_3 as fluxing agent and B was extracted after adding ultrapure water and passing the solution through anion and cation exchange columns. Full detailed description of methods, errors and analyses of reference materials can be found in Innocenzi et al. (2021, 2024) and Agostini et al. (2021, 2022).

4. Results

In the next paragraphs, the main petrographic, mineral chemical, geochemical and isotopic features are reported. Further information and diagrams can be found in the Supplementary material 1 and 2.

4.1. Petrography

Samples MF3, MFF4 and MFF6 (Forcinella lava flow) are porphyritic and weakly scoriaceous lavas, with a hypo-holocrystalline groundmass (Fig. 2a-b). Vesicles (2 to 15 vol%) are commonly irregular in shape, mostly less than ~2 mm in size, and occasionally partially to totally filled by zeolites (e.g., sample MFF6). Phenocrysts (<3 mm in size) define a Porphyricity Index (P.I., i.e., the area occupied by the phenocrysts over the total area of the thin section, excluding voids) in the ~10–15 vol% range. They are mostly anhedral to euhedral clinopyroxene and subhedral to euhedral leucite, whose occasional fractures are filled by either calcite or zeolites. Colourless to light green or light yellow clinopyroxene phenocrysts exhibit a corroded and irregular habit. They are often surrounded by melilite (samples MF3 and MFF6) or by a fine-grained, optically unresolvable reaction corona (samples MF3 and MFF4; Fig. 2c-d). Sample MFF4 is richer in poikilitic leucite phenocrysts (40–50 vol%) with inclusions of subhedral clinopyroxene. The groundmass is made up of anhedral to euhedral laths of light green to yellow clinopyroxene, zoned melilite (up to 10–15 vol%) either fresh (in samples MFF6 and MF3) or altered (in sample MFF4), euhedral leucite, intergranular phlogopite, anhedral nepheline and kalsilite, rare euhedral apatite and subhedral opaques (Fig. 2a-b). Kalsilite is a relatively abundant phase in sample MF3 (~5–8 vol%; Fig. 3), while lower modal amounts are observed in other samples. Rare, partially zeolitized, glass is found in samples MFF4 and MMF6. Samples MF3 and MFF6 contain carbonate plagues (<1 mm in size), including green and corroded clinopyroxene and nepheline (Fig. 2e-f).

Samples from the Feltricci lava flow (samples MF4, MFF7, MFF9, MFF10, MFF11, MFF12 and MFF13) range from subaphyric to weakly porphyritic (MFF7 P.I. = 8–10 vol%) to porphyritic and glomeroporphyritic (MF4, MFF9, MFF10, MFF11, MFF12 and MFF13; P.I. = 10–15 vol%). They span from weakly vesicular (MFF12 and MFF13; 5% vesicles) to highly vesicular samples (MFF9 and MFF10; 15–25 vol% vesicles). Vesicles are empty and variably shaped (sub-rounded or irregular to almost isooriented and elongated) and with a size ranging from ~2 to ~8 mm. The main difference with respect to the Forcinelle lava samples is the higher modal abundance of olivine (up to 10 vol%), found as subhedral to euhedral phase as phenocrysts and/or groundmass microliths. In both cases, olivine is partially iddingsitised. Other and more abundant phenocrysts (<2 mm) are light green to colourless, subhedral to euhedral clinopyroxene. Rare, zoned clinopyroxene phenocrysts with a green rim and colourless core are also found. The hypocrystalline to holocrystalline groundmass is fine-grained and partially altered. It consists of euhedral twinned leucite, euhedral olivine, euhedral to subhedral, light green to light yellow clinopyroxene, rare anhedral phlogopite, nepheline and/or kalsilite, anhedral and poikilitic melilite, found as fresh phase, also showing peg structures, or altered yellowish patches (much more abundant in sample MF4 than in the others), anhedral to euhedral apatite and subhedral to euhedral opaques. Rare intergranular yellow volcanic glass may also be present. In sample MFF12, primary carbonate plagues, hosting clinopyroxene and leucite microphenocrysts, can also be observed (Fig. 2g-h).

4.2. Mineral chemistry

Mineral and glass chemical analyses have been carried out on five of the most representative and freshest samples (samples MF3 and MFF4 from the Forcinella lava, samples MF4, MFF12 and MFF13 from the Feltricci lava). All the data and classification diagrams are reported in the Supplementary material 2 (Mineral and glass chemistry).

Olivine is a common phase in the Feltricci lava flow (samples MF4, MFF12 and MFF13) occurring either as phenocryst or in the groundmass, whereas in sample MF3 (Forcinella lava flow) only one microphenocryst has been found. Olivine phenocrysts and microphenocrysts from the Feltricci samples show higher Fo (0.84–0.89) and slightly lower CaO (0.71–1.31 wt%) than groundmass phases (Fo = 0.56–0.86; CaO = 0.93–1.56 wt%). On the other hand, the olivine microphenocrysts from Forcinella sample MF3 have lower Fo (~0.78–0.80) and similar CaO (1.08–1.54 wt%) abundances. NiO content for olivine in sample MF3 (0.01–0.05 wt%) shows slightly lower values with respect to the Feltricci lava (0.08–0.14 wt% for phenocryst and 0.09–0.24 wt% for the groundmass). The key feature of this mineral is the significantly high content of CaO, which is higher than the values of the other Roman Province plagio-leucitites (0.31–0.55 wt%; Ammannati et al., 2016), but comparable with San Venanzo (IAP) kamafugite (1.71 wt%; Lustrino et al., 2020).

Clinopyroxene is a ubiquitous phase in both lava flows, with all the analyses falling in the diopside field but showing a relevant Ca-excess (phenocrysts cores $En_{42-47}Fs_{3-5}Wo_{49-54}$ and rim $En_{35-46}Fs_{0-4}Wo_{51-57}$, groundmass $En_{38-45}Fs_{3-11}Wo_{52-57}$). All the clinopyroxenes show a variable Si deficiency in the tetrahedral sites, which is generally compensated by the presence of ^{IV}Al. Clinopyroxene compositions for the Feltricci lava (MF4 and MFF12) show a quite continuous trend with a

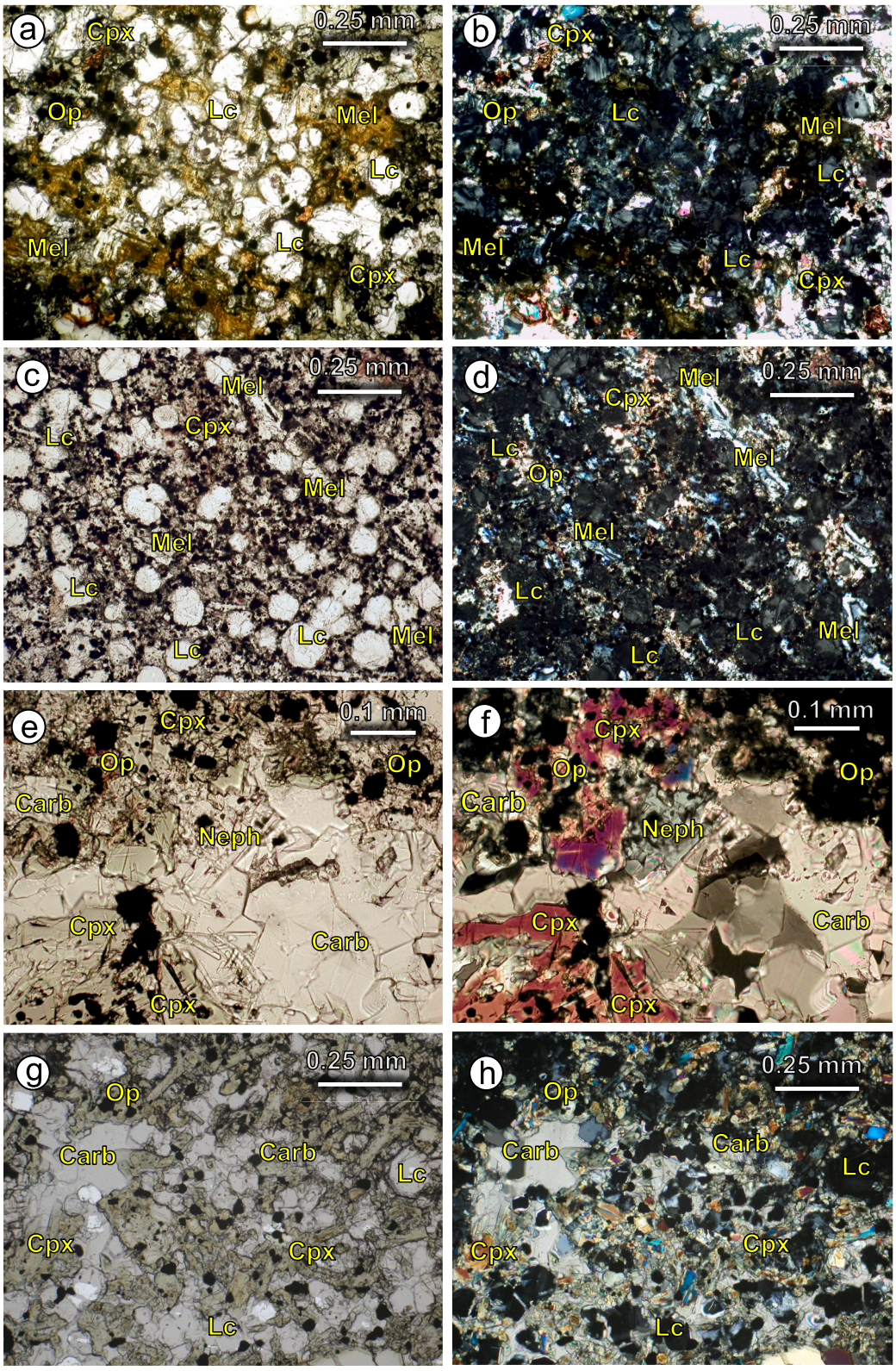

Fig. 2. Photomicrographs of Forcinella and Feltricci samples (on the left plane polarized light and on the right crossed polarized light). a-b) sample MF4 (Feltricci lava flow): groundmass of the porphyritic lava, with altered and fresh melilite, leucite, clinopyroxene and opaques microphenocrysts and microliths. c-d) sample MFF6 (Forcinella lava flow): euhedral microphenocryst of melilite and leucite. e-f) samples MF3 (Forcinella lava flow): carbonate plague in the groundmass of a melilite- and kalsilite-bearing lava including subhedral clinopyroxene and nepheline. g-h) samples MFF12 (Feltricci lava flow): groundmass carbonate plague of a melilite- and kalsilite-bearing lava, containing subhedral to euhedral clinopyroxene, nepheline and leucite. Carb = carbonate, Cpx = clinopyroxene, Lc = leucite, Mel = melilite, Neph = nepheline, Op = opaque phases.

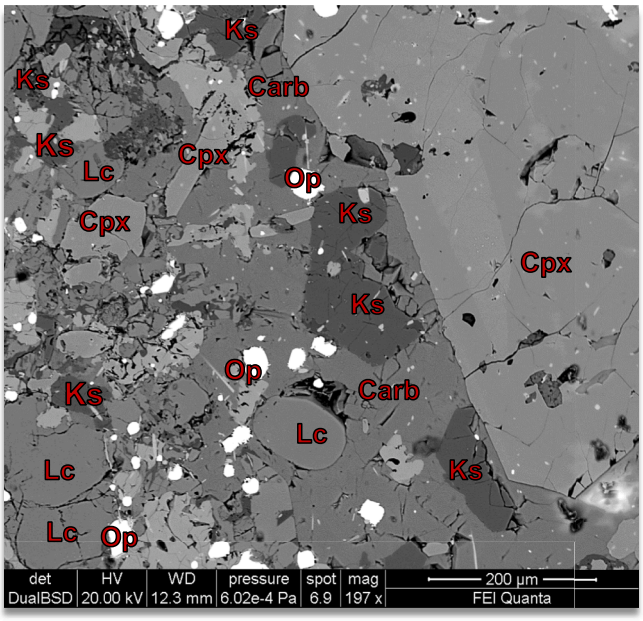

Fig. 3. SEM microphotograph of the groundmass of sample MF3 (Forcinella lava), highlighting the various mineral phases. Carb = carbonate, Cpx = clinopyroxene, Lc = leucite, Neph = nepheline, Ks = kalsilite, Op = opaque phases.

general decrease in Si and Mg and an increase of Al, Ti, Fe and Na from phenocryst cores to phenocryst rims and the groundmass microliths. However, compared to the Feltricci clinopyroxenes, those from Forcinella (samples MF3 and MFF4) show a higher Si deficiency, lower Mg contents, higher Fe, Na and Ti (Supplementary material 2). Clinopyroxene occurring in the carbonate plagues shows compositions comparable to groundmass clinopyroxene, with high Na and Ti. Chromium contents are generally low (Cr_2O_3 < 0.13 wt%), except from some phenocrysts in Forcinella sample MF4 (up to 0.58 wt%).

Melilite is a common phase in Forcinella lava flow, while it has only been found in some of the samples from Feltricci (MF4, MFF10, MFF12 and MFF13). All the analysed crystals are enriched in the åkermanite component [$Ca_2MgSi_2O_7$ = 52.1–63.9%], soda melilite [$CaNa(Al, Fe^{3+}, Ti)Si_2O_7$ = 18.1–25.8%] and iron åkermanite [$Ca_2(Fe^{2+}, Mn)Si_2O_7$ = 8.3–16.7%]. Lower components are the Na ferrimelilite [$CaNaFe^{3+}Si_2O_7$ < 4.1%] and iron gehlenite [$Ca_2Fe^{3+}(AlSiO_7)$ <4.6%] end-members. SrO and Cr_2O_3 contents are always low (<1.05 wt% and < 0.04 wt%, respectively). Only minimum amounts of Al_2O_3 are required to fill the tetrahedral site (^{IV}Al < 0.091 apfu).

Leucite is ubiquitous both as euhedral phenocrysts and as microphenocrysts. The K# value [100*K/(K + Na)], varies between 98 and 100, close to almost pure potassic compositions, with BaO reaching values up to 0.65 wt%.

Kalsilite occurs as a groundmass phase only, modally abundant in sample MF3, but <5–8% in MF4 and MFF4 samples (e.g., Fig. 3). SEM analyses highlighted the occurrence of kalsilite also in other Feltricci lavas (as MFF7, MFF9, and MFF12). Kalsilite samples MF3 (Forcinella), MF4 and MFF12 (Feltricci) show similar compositional ranges, with values of Kal comprised between 85.6 and 92.7 [Kal = 100*Ks/(Ks + Ne + Sil), where Ks = K, Ne = Na and Sil = Si-(2*Ca + Na + K)]. Kalsilite from Forcinella sample MFF4 shows lower Kal values (77.1), due to the slightly lower K_2O (23.9 wt%) and higher Na_2O (2.3 wt%) with respect to kalsilite crystals from samples MF3 (Na_2O = 0.6–0.7 wt%), MF4 (Na_2O = 0.4 wt%) and MFF12 (Na_2O = 0.9–0.15 wt%).

Nepheline is a common groundmass phase characterized by a Ne [100*Ne/(Ks + Ne + Sil)] ranging from 54.7 (Feltricci sample MFF13) to 72.8 (Feltricci sample MFF12). This mineral is enriched in potassium, with K_2O ranging from 8.0 to 9.5 wt% and Na# value [100*Na/(Na + K)] ranging from 59.4 to 69.9. BaO is negligible (<0.05 wt%).

Phlogopite occurs in the groundmass of both lava flows as intergranular phase with high Mg# [Mg/(Mg + Fe^{2+})] values ranging from 0.8 to 0.9 and low SiO_2 (<37.7 wt%). The Si deficiency (Si = 2.701–2.831 apfu, on the basis of 22 anions) allows ^{IV}Al (1.156–1.299 apfu) and occasionally also Fe^{3+} (0.013 apfu) to enter the tetrahedral site. BaO and F content are always high (5.4–9.3 wt% and 5.9–6.6 wt%, respectively). TiO_2 increases from 1.25 to 1.57 wt% in the Feltricci samples to 2.21 wt% in the Forcinella samples, whereas FeO has the opposite trend (4.90–5.80 wt% in Forcinella samples and 6.65–7.10 wt % in Feltricci samples).

Carbonates are found in some segregation plagues occurring in the groundmass and hosting silicate minerals (Fig. 5). The carbonate shows no BaO (<0.01 wt%) and SrO ranging from <0.01 wt% (Forcinella sample MF3) to 1.20–1.89 wt% (Feltricci sample MFF12), coupled with nearly pure calcite composition (FeO = 0.04–0.14 wt%; MgO = 0.04–0.88 wt%).

Spinels are found in all samples as subhedral to euhedral groundmass phases. All spinels belong to the magnetite-ulvöspinel series (FeO_{tot} = 69.9–82.6 wt%; Fe^{3+} = 1.041–1.428 apfu; Fe^{2+} = 0.885–1.227 apfu, based on 4 oxygens and 3 cations). The spinel analysed in Forcinella samples have higher ulvöspinel component (Usp = 0.30–0.39) compared with those from the Feltricci samples (Usp = 0.14–0.24).

4.3. Whole-rock geochemistry

The composition of the five most representative samples (MF3 and MFF6 from Forcinella lava flow, plus samples MF4, MF10 and MF12 from Feltricci lava flow) are reported in Table 1, whereas a comparison of the new data with literature samples and several diagrams are reported in the Supplementary material 1. On the TAS diagram (Fig. 4), Forcinella lavas fall in the foidite field, with 42.1–42.6 wt% SiO_2 and Na_2O + K_2O in the 9.6–10.1 wt% range. On the other hand, Feltricci lavas fall in the basanite/tephrite field (SiO_2 = 45.6–45.9 wt% and 6.9–7.8 wt% total alkali, with CIPW normative olivine <10% for MF4, and > 10% for MFF10 and MFF12). Despite this, Feltricci rocks cannot be classified as real basanites/tephrites as they lack plagioclase. All the samples are characterized by high Al_2O_3, CaO and K_2O, with very low TiO_2 and Na_2O (Table 1). Forcinella lava is characterized by lower Mg# (0.54–0.55) than Feltricci lava (0.67–69; calculated with $Fe_2O_3/\Sigma Fe$ ratio = 0.15). The new samples plot within the literature field for Montefiascone products, showing an ultrapotassic affinity, being characterized by MgO and K_2O > 3 wt%, coupled with K_2O/Na_2O > 2 (5.30–6.79 for Forcinella lava and 5.30–8.72 for Feltricci lava; Foley et al., 1987; Supplementary material 1).

Harker diagrams of some major oxides (Al_2O_3, Fe_2O_3, CaO and K_2O) vs. MgO (Fig. 5), exhibit a rough alignment of the Montefiascone lavas from this study with the general trend described by IAP products, from San Venanzo to Cupaello and Oricola (see also Supplementary material 1). The Feltricci and Forcinella lavas only partially overlap the bulk of the Montefiascone literature samples, showing more similarities with IAP products (Fig. 5 and Supplementary material 1).

Samples from Forcinella lava are variably enriched in incompatible trace elements such as LILE and REE, with strong depletion of HFSE (Supplementary material 1). Feltricci lavas show lower incompatible trace element contents compared to the Forcinella rocks. Again, a strong similarity between the samples from this study and literature samples from Alban Hills and IAP rocks (only San Venanzo and Cupaello) emerges (Fig. 5 and Supplementary material 1). Most of the incompatible trace elements (e.g., Ba and LREE) are slightly less enriched in the Montefiascone samples than in the Alban Hills and IAP (especially Cupaello volcano; Fig. 5).

The incompatible element abundances normalised to the primitive mantle estimate (Fig. 6a) evidence a spiky pattern showing marked negative anomalies at Ba, Nb, P and Ti, coupled with peaks for Th, U and Pb. CI chondrite-normalised (Fig. 6b) REE patterns are LREE enriched

Table 1
Whole rock compositions for major and trace elements of volcanic products from Montefiascone Volcanic Complex.

	Forcinella lava		Feltricci lava		
Sample	MF3	MFF6	MF4	MFF10	MFF12
SiO_2	42.63	42.15	45.94	45.93	45.56
TiO_2	0.90	0.86	0.77	0.78	0.77
Al_2O_3	14.19	14.53	12.71	13.16	12.76
$Fe_2O_{3(total)}$	8.99	8.70	8.68	8.76	8.69
MnO	0.16	0.15	0.15	0.15	0.15
MgO	4.76	4.40	7.59	8.03	8.28
CaO	15.09	14.88	13.98	14.43	14.85
Na_2O	1.60	1.23	1.04	0.71	1.24
K_2O	8.48	8.35	6.17	6.19	6.57
P_2O_5	0.72	0.70	0.42	0.45	0.43
L.O.I.	2.22	3.55	1.64	1.82	0.90
Total	99.74	99.50	99.08	100.40	100.20
Mg#	0.55	0.54	0.67	0.68	0.69
Rb	583	636	481	404	398
Sr	2423	2492	820	962	1281
Ba	1703	1697	1178	1242	1165
Cs	48.4	45.8	34.7	29.9	29.3
Sc	14	12	29	30	30
V	280	272	262	270	254
Cr	20		230	210	220
Co	29	28	38	35	35
Ni	50	50	120	110	110
Cu	100	100	130	120	120
Zn	80	80	60	70	70
Y	40	38	30	33	32
Zr	397	386	238	268	265
Nb	20	19	11	10	10
Hf	5.8	6.5	6.8	6.2	6.1
Ta	0.9	0.8	0.5	0.4	0.4
La	164	162	96.5	91.3	87.9
Ce	337	329	196	187	184
Pr	39	38.1	23.5	22.8	22.4
Nd	152	144	92.7	89.8	87.3
Sm	26.5	25.2	18.1	17	16.7
Eu	4.93	4.67	3.42	3.16	3.17
Gd	15.8	15.1	11.6	11.5	11.5
Tb	2	2	1.5	1.5	1.4
Dy	9.3	8.7	7.4	6.8	6.8
Ho	1.4	1.4	1.2	1.1	1.1
Er	3.4	3.3	2.8	2.5	2.5
Tm	0.43	0.41	0.35	0.34	0.35
Yb	2.6	2.4	2.1	2.2	2.0
Lu	0.37	0.38	0.34	0.31	0.3
Pb	77	69	43	51	28
Th	69.4	66.4	33.5	34.5	33.6
U	16	15.8	6.6	7.1	8.2
Ga	18	17	15	16	15

(La = 400–700 x chondrite) and exhibit significant LREE/HREE fractionation, with $(La/Lu)_N$ ratios ranging from 30.4 to 47.5, coupled with slight negative Eu anomalies (Eu/Eu* = 0.69–0.73). The two Montefiascone lava flows show extremely similar patterns, but Forcinella samples are more REE enriched than those from the Feltricci lava.

4.4. Isotope geochemistry (Sr-Nd-Pb-B)

Radiogenic (Sr-Nd-Pb) and stable (B) isotopic ratios have been analysed on the three most representative samples (i.e., MF3, MF4 and MFF6; data on Table 2 and Supplementary material 1). Considering the young age of the samples (<286 ka; Brocchini et al., 2000), and the low Rb/Sr, Nd/Sm, U/Pb and Th/Pb ratios, no age correction was performed. Strontium isotopes ratios are extremely radiogenic, always much higher than the BSE (Bulk Silicate Earth) $^{87}Sr/^{86}Sr$ values, ranging between 0.71039 and 0.71042 for Forcinella lava and 0.71068 for Feltricci lava (Fig. 7a-b). In a similar way, the $^{143}Nd/^{144}Nd$ ratios are much lower than the ChUR (Chondritic Uniform Reservoir), pointing to an enriched component, ranging between 0.512057 (Feltricci lava) and 0.512074–0.512091 (Forcinella lava; Fig. 7a-b). Values for Sr and Nd isotopic ratios completely overlap the literature fields of Montefiascone and IAP (in particular San Venanzo) volcanic rocks. Lead isotopic ratios for the Montefiascone lavas are radiogenic, with $^{206}Pb/^{204}Pb$ ranging between 18.76 and 18.78, $^{207}Pb/^{204}Pb$ = 15.68 and $^{208}Pb/^{204}Pb$ between 38.98 and 39.02 (Fig. 7d-e). The $^{206}Pb/^{204}Pb$ and $^{208}Pb/^{204}Pb$ ratios of the new samples overlap the scarce literature data of Montefiascone rocks (18.73–18.78 and 38.94–39.01, respectively) but are more radiogenic than the literature $^{207}Pb/^{204}Pb$ ratios (15.65–15.66). Also in this case, the Forcinella and Feltricci Pb isotopes share more similarities with IAP rocks. As concerns mantle end-member compositions, the Forcinella and Feltricci samples plot outside the DMM-HIMU-EMI-EMII quadrilateral in terms of Sr—Nd isotopic compositions, whereas the same samples plot very close to the EMII end-member, far away from EMI, DMM and HIMU compositions (e.g., Lustrino and Anderson, 2015).

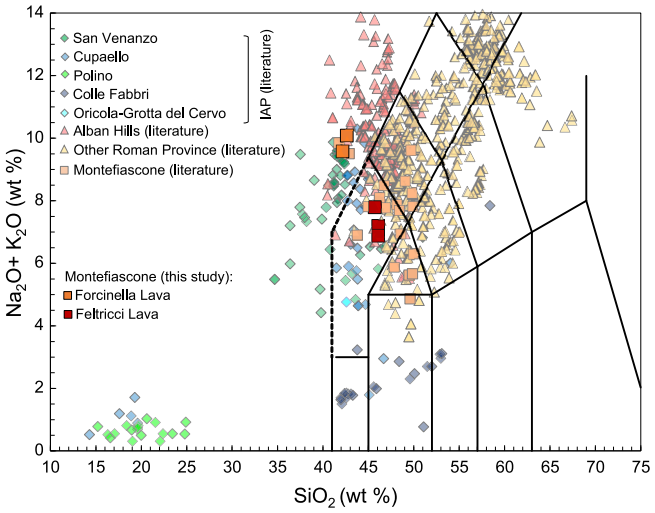

Fig. 4. TAS diagram (Le Maitre, 2002) showing the compositions of Forcinella and Feltricci samples from this study compared with data from literature for the Roman Province (i.e., Vico, Vulsini Mts. and Sabatini Mts.), Montefiascone Volcanic Complex, Alban Hills and IAP. All details and references are reported in the Supplementary material 1.

The $\delta^{11}B$ shows negative values varying between −7.36 and −8.82‰. These values roughly match with the DMM range (−6 to-8‰) and fall within the OIB range (−5 to −10‰; Agostini et al., 2021 and references therein). Being the boron isotopic systematic not yet widely applied to volcanics rocks worldwide, only a few data for central Italy are available in literature: some whole rock data analysed with the same method of data presented here (Innocenzi et al., 2023, Fig. 7f) and some other laser ablation analyses via SIMS on melt inclusions (Luciani et al., 2023). The data presented in this study overlap with the whole-rock values from IAP (from −7.54 to −8.80‰; Innocenzi et al., 2023; Innocenzi, 2024), but are strongly different from the melt inclusions $\delta^{11}B$ of Vulsini Mts. (from −10.6 to −21.1‰), IAP (from −24.5 to −29.2‰) and Alban Hills (from −8.5 to −18.3‰) reported by Luciani et al. (2023).

5. Discussion

The Quaternary alkaline potassic and ultrapotassic magmatism from central Italy has always grabbed the attention of Earth scientists, because of its extreme composition and the complex geodynamic settings in which such magmatic activity developed (e.g., Lustrino et al., 2022a). The kalsilite- and melilite-bearing lavas from the Montefiascone Volcanic Complex analysed in this study, represent ultrapotassic rocks, sharing several mineralogical and geochemical features with the Alban Hills potassic and ultrapotassic products (see Fig. 5 and Supplementary material 1), but also with the rarer kamafugitic volcanic rocks of the IAP.

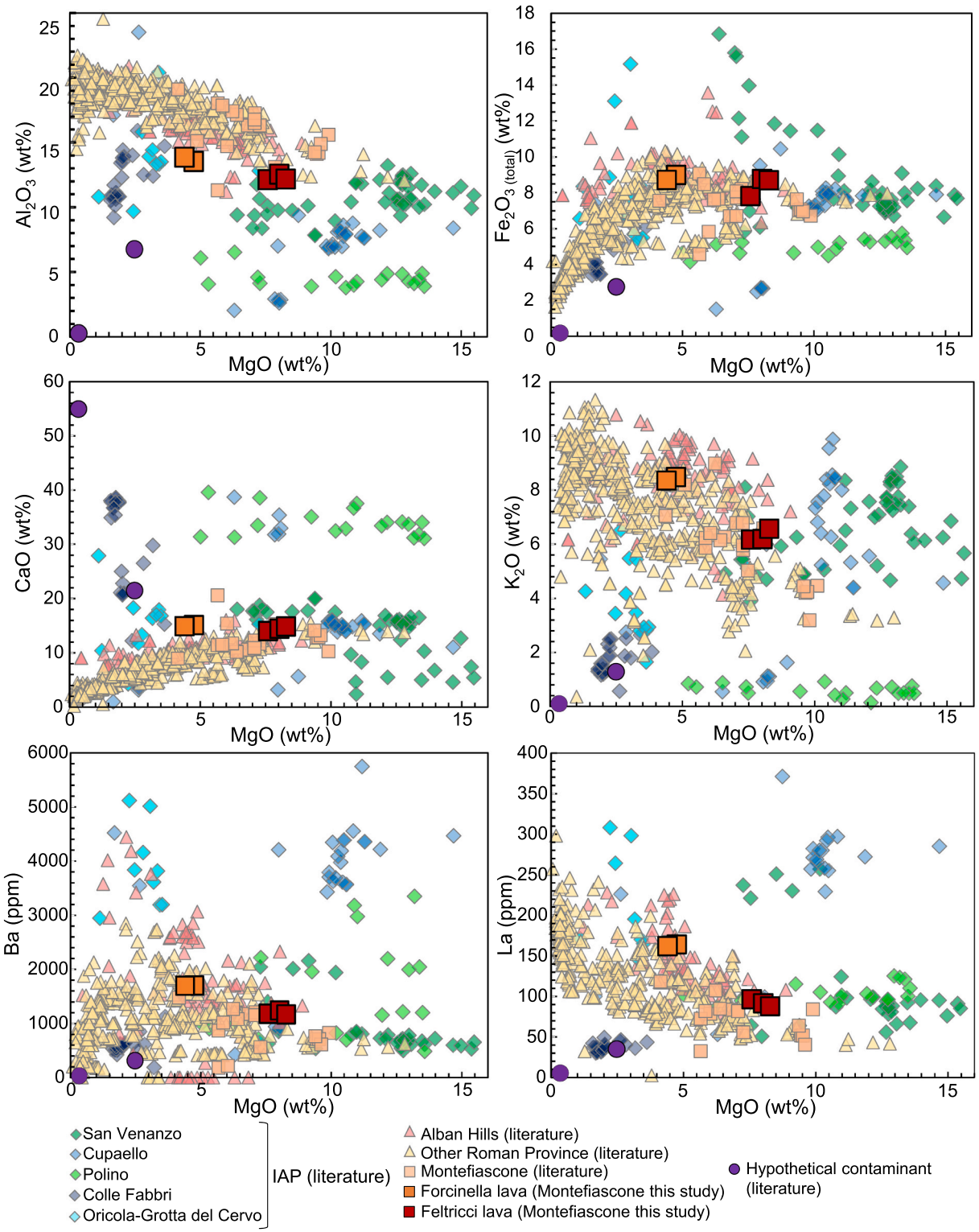

Fig. 5. Harker diagrams for selected major oxides and trace elements vs. MgO. Data from literature for the Vulsini Mts., Sabatini Mts., Vico (other Roman Province), Alban Hills and IAP are reported for comparison. References are reported in Supplementary Material 1. The plotted contaminant compositions are a limestone (Maiolica formation) (Lustrino et al., 2022) and an early Miocene pre-flysch marl (Lustrino et al., 2020).

Therefore, this study can contribute to achieve a better understanding of these peculiar compositions and their petrogenesis, as well as to define their relationship with the other central Italy Quaternary volcanic districts.

5.1. *Petrographic and mineral chemical constraints*

The mineral paragenesis is slightly variable between the two investigated lava flows but also within the single flows. Kalsilite is a groundmass component in both outcrops, but its modal abundance varies from <2% (sample MF4) to ~5–8% (samples MF3). Nevertheless,

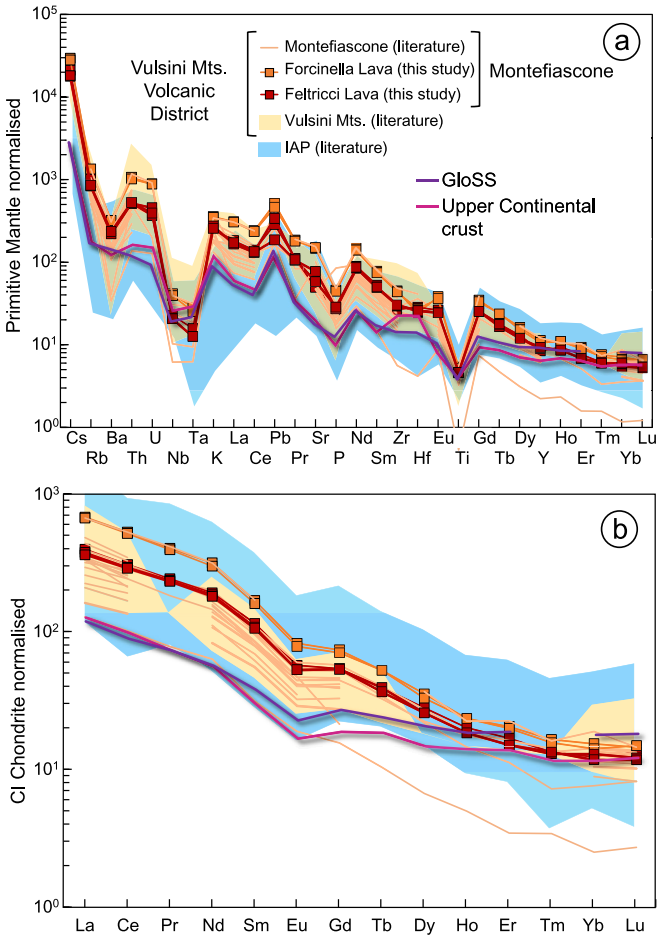

Fig. 6. a) Primitive mantle-normalised incompatible element diagrams for lava samples from Montefiascone Volcanic Complex. Primitive mantle values from Lyubetskaya and Korenaga (2007). b) CI chondrite-normalised patterns for REE for the lava samples from Montefiascone Volcanic Complex. CI chondrite composition is from King et al. (2020). Literature field described by Vulsini Mts. samples, together with IAP rocks are also plotted. References are reported in Supplementary Material 1. GloSS composition from Plank (2014) and Upper continental crust average from Rudnick and Gao (2014).

some of the Feltricci samples (e.g., sample MFF7) show a very fine-grained groundmass, where the identification of late intergranular phases and their abundances is particularly difficult to evaluate. This means that the effective content of kalsilite, which is one of the last minerals to crystallize in these systems, could be even higher than 10%. Besides kalsilite, nepheline and leucite are the two other foids in the Feltricci and Forcinella lavas. Leucite is always more abundant than nepheline, reaching 30–40 vol% in samples MFF4, found either as phenocrysts and as groundmass phase. Two other key features to be reported are the absence of any feldspar in the investigated rocks and the presence of particularly CaO-rich olivine.

Di Battistini et al. (2001) classified the Feltricci and Forcinella lavas as leucite melilitites. Considering the finding of anhedral groundmass kalsilite, the rocks should be more properly classified as kalsilite-bearing rocks, following the IUGS criteria (Le Maitre, 2002).

The high CaO content in olivine (0.71–1.56 wt%), which also largely exceeds the range observed for olivine from central Italy leucitites Fig. 8), may be due to an intense mantle metasomatism, caused by the presence of a carbonate component. The ultimate effect of this infiltration could be a partial to complete reaction with the matrix peridotite, resulting in a strong depletion in orthopyroxene and increase of modal clinopyroxene (e.g., Ammannati et al., 2016). The absence of orthopyroxene in a wehrlite source could explain the low silica content of the produced melts, whereas the high modal abundance of clinopyroxene in the source, possibly coupled with modal carbonates, would explain the overall high CaO budget of the rocks (as well as of olivine crystals).

Another interesting feature of Forcinella and Feltricci lavas is the presence of groundmass carbonate plagues hosting euhedral silicate phases such as nepheline and clinopyroxene (Fig. 2e-h; Fig. 9). Such plagues, clearly representing pockets of carbonate-rich residual melts, may provide hint for a carbonate-veined mantle source, but can also ultimately result from sedimentary carbonate assimilation at shallow depths, as already proposed for other IAP volcanoes such as Polino (Lustrino et al., 2019; Peccerillo, 1998) and San Venanzo (Lustrino et al., 2020). The hypothesis of a shallow origin for the carbonate component is strengthened by the chemical composition of these carbonate plagues, characterized by BaO and SrO contents close to detection limit, very low MgO and FeO, much closer to sedimentary limestones than to carbonates formed in a peridotitic matrix.

In addition, these late-forming carbonate plagues are frequently coupled with reaction rims (often made by melilite) around clinopyroxene phenocrysts (especially in the Forcinella samples) and abundant melilite and kalsilite crystallizing as groundmass phases, pointing out a variation in the composition of the residual melt, especially in terms of SiO_2 undersaturation.

Lustrino et al. (2022b) related the presence of melilite rims around clinopyroxene in kamafugite lavas from Cupaello volcano to the assimilation of sedimentary lithologies by an ultrabasic melt. Innocenzi et al. (2024) explained similar petrographic features in Ugandan kamafugites invoking $CaCO_3$-bearing veins in the source, which would have produced melts enriched in carbonate component. On the other hand, the crystallization of phenocryst phases, such as olivine and leucite, plus minor clinopyroxene, would ensure a residual melt enriched in carbonate (either CaO and CO_2).

As previously stated by Di Battistini et al. (2001), shallow crustal contamination cannot be ruled out for the two Montefiascone lava flows considering the presence of limestone-rich lithologies in the sedimentary substrate of the volcanic area. The overall low volume of the emplaced magma could result in a high sedimentary carbonate/magma ratio during magma upwelling, favouring basement limestone and marly limestone assimilation in shallow depth crustal chambers. Worth noting, however, geochemical (e.g., the enrichment in trace elements) and isotopic data (strongly radiogenic Sr) are not entirely consistent with a significant sedimentary carbonate assimilation, considering that these crustal lithologies are nearly sterile in terms of incompatible element budget and characterized by much less radiogenic Sr isotopic compositions. Indeed, the process of a simple limestone assimilation would have resulted in an incompatible element dilution in the hybrid magma, as

Table 2
Radiogenic ($^{87}Sr/^{86}Sr$, $^{143}Nd/^{144}Nd$, $^{206}Pb/^{204}Pb$, $^{207}Pb/^{204}Pb$, $^{208}Pb/^{204}Pb$) and stable ($\delta^{11}B$) isotopic ratios of volcanic products from Montefiascone Volcanic Complex.

Sample	$^{87}Sr/^{86}Sr$	$^{143}Nd/^{144}Nd$	$^{206}Pb/^{204}Pb$	$^{207}Pb/^{204}Pb$	$^{208}Pb/^{204}Pb$	$^{208}Pb/^{206}Pb$	$^{207}Pb/^{206}Pb$	Δ7/4	Δ8/4	$\delta^{11}B$
Forcinella lava										
MF3	0.710418	0.512091	18.758	15.680	39.018	2.080	0.836	15.5	71.2	−7.36
MFF6	0.710385	0.512074	18.757	15.680	39.017	2.080	0.836	15.6	71.2	−8.05
Feltricci lava										
MF4	0.710678	0.512057	18.780	15.678	38.984	2.076	0.835	15.1	65.2	−8.82

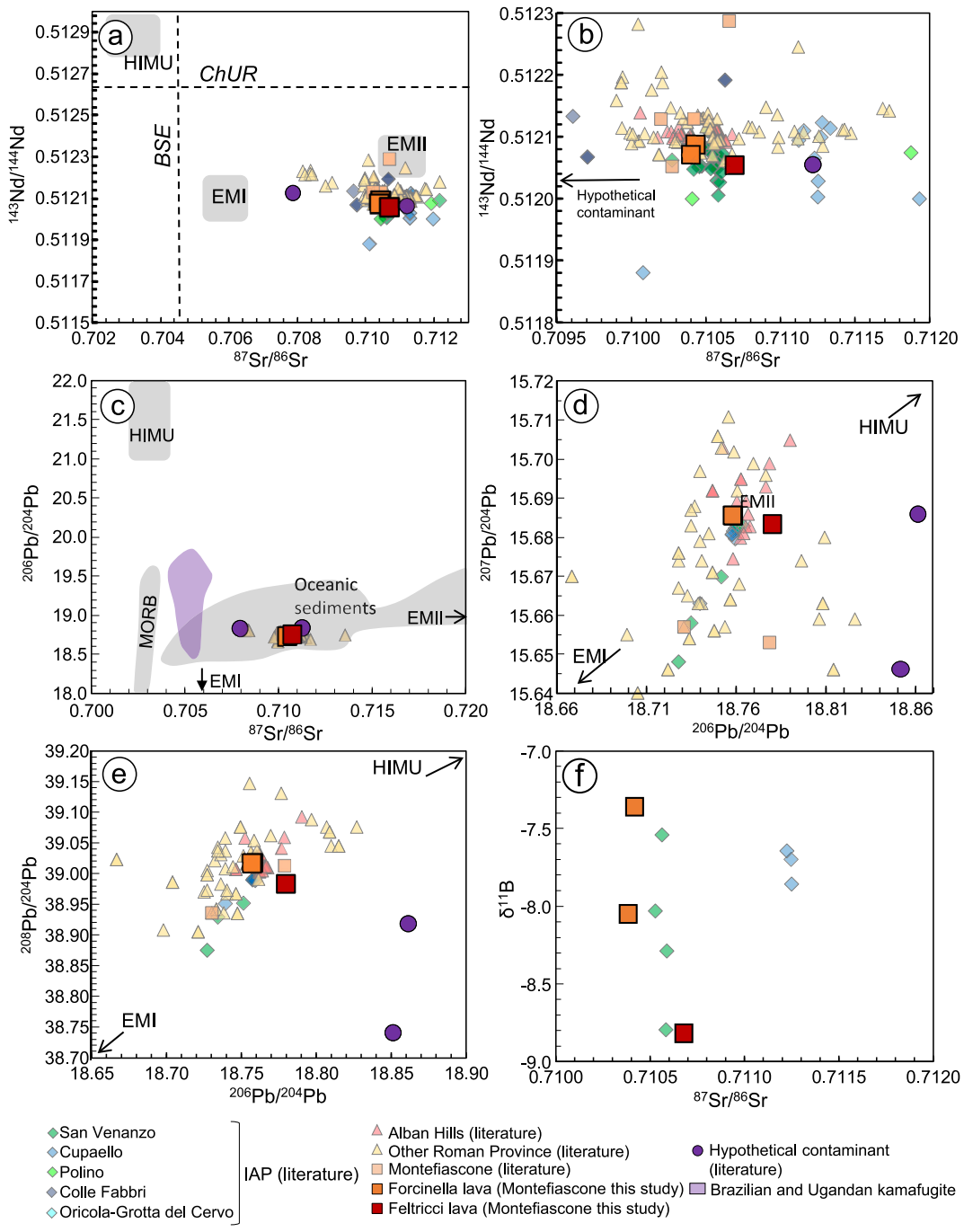

Fig. 7. Radiogenic isotopic data plotted on Harker diagram: a) $^{143}Nd/^{144}Nd$ vs. $^{87}Sr/^{86}Sr$ diagram. b) close-up view of the $^{143}Nd/^{144}Nd$ vs. $^{87}Sr/^{86}Sr$ diagram. c) $^{206}Pb/^{204}Pb$ vs. $^{87}Sr/^{86}Sr$. d) $^{207}Pb/^{204}Pb$ vs. $^{206}Pb/^{204}Pb$ diagram. e) $^{208}Pb/^{204}Pb$ vs. $^{206}Pb/^{204}Pb$. f) $\delta^{11}B$ vs. $^{87}Sr/^{86}Sr$. Sample MF3, MF4 and MFF6 are plotted together with the literature data for Roman Province and IAP. References are reported in Supplementary Material 1. EMI = Enriched mantle I, EMII = Enriched mantle II, HIMU = High-μ, from Lustrino and Anderson, 2015 and references therein. Data for Brazilian and Ugandan kamafugites are from Innocenzi (2024) and reference therein.

well as $^{87}Sr/^{86}Sr$ isotopic ratios not higher than 0.70800 (Di Battistini et al., 2001).

5.2. Geochemical and isotopic considerations on the mantle source

The analysed kalsilite- and melilite-bearing lavas from Montefiascone Volcanic Complex are young lithotypes (<286 ka; Brocchini et al., 2000), with low L.O.I. (0.9–3.55) and barely altered (i.e., zeolites are found only in vesicles and fractures and do not replace any groundmass phase). Therefore, we consider that these rocks have not been strongly affected by post-emplacement remobilization of both major and trace elements. They are ultrabasic to basic compositions, coupled with high CaO and ultrapotassic affinity (Figs. 3 and 4; Supplementary material 1). Nevertheless, Forcinella and Feltricci lavas slightly differ from a geochemical point of view too, as Forcinella has a slightly more evolved character, with lower Mg# (0.54–0.55) compared to Feltricci (0.67–0.69), coupled with higher CaO (~14.9–15.1 wt% vs. 14.0–14.9) and K_2O (~8.4–8.5 wt% vs. 6.2–6.6 wt%). A slightly different fractionation history could be assumed to explain such subtle differences (see next section).

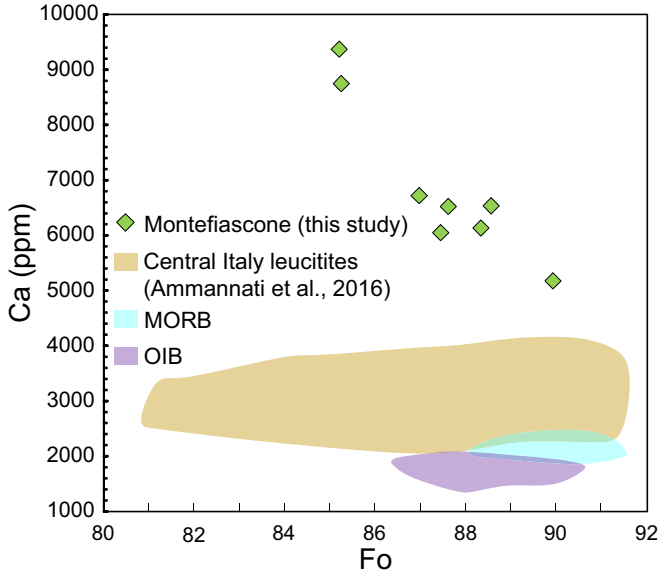

Fig. 8. Harker diagram for Ca (ppm) vs. Fo content of olivine phenocrysts and microphenocrysts from this study. The orange, the blue and the purple fields are respectively for olivine crystals from central Italy leucitites, MORBs and OIBs (from Ammannati et al., 2016 and references therein). (For interpretation of the references to colour in this figure legend, the reader is referred to the web version of this article.)

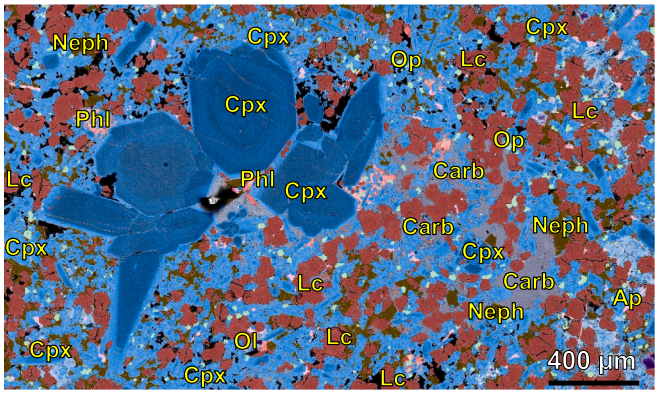

Fig. 9. FE-SEM maps of a carbonate plague from lava sample MFF12. Dark blue mineral is diopside, light blue augite, light red is phlogopite, violet is olivine, brown is nepheline, dark red is leucite, grey is calcite, pink is apatite and green is magnetite. Carb = carbonate, Cpx = clinopyroxene, Lc = leucite, Neph = nepheline, Ol = olivine, Op = opaque phases, ap = apatite and phl = phlogopite. (For interpretation of the references to colour in this figure legend, the reader is referred to the web version of this article.)

Although the Montefiascone rocks derived from differentiated magmas (see next paragraph), the general geochemical signature (e.g., the high CaO and K_2O contents) seems to be inherited by the parental melts. As proposed for the other ultrabasic and ultrapotassic products worldwide, pervasive metasomatic processes need to have permeated their mantle sources, probably producing to a non-peridotitic assemblage. Davis et al. (2011) demonstrated experimentally that primitive magmas with total alkali >4 wt% require low degree of partial melting of metasomatized lherzolite source. Therefore, mineral phases different from those forming a typical mantle assemblage must be involved to cause these alkali-rich compositions. As already evidenced, the high CaO and the slightly ultracalcic nature of Montefiascone samples (CaO/Al_2O_3 = 1.02–1.10) of Feltricci and Forcinella lavas, coupled with their strongly SiO_2-undersaturated composition require a carbonated source enriched in clinopyroxene. In addition, to explain the very high K_2O content and the radiogenic Sr isotopic ratios, the presence of ancient Rb-rich phlogopite is also required. The extremely low TiO_2 and P_2O_5 suggest a metasomatic agent either poor in these elements or the presence of restitic accessory minerals such as apatite and titanates or the early fractionation of these minerals during magma evolution.

A lithospheric mantle source metasomatized by the interaction with subducted lithologies (e.g., terrigenous sediments), is supported by the incompatible element fractionation (e.g., high LILE and REE, coupled with high LILE/HFSE ratios; Fig. 6a). To provide further support to this model the compositions of GloSS (Global Subducting Sediments; Plank, 2014), and the average value for the upper continental crust (Rudnick and Gao, 2014), have been plotted in Fig. 6a. Both compositions closely resemble the interelemental fractionation of the Montefiascone samples, sharing negative and positive anomalies. The negative Eu anomalies observed in CI chondrite-normalised REE patterns (Fig. 6b) are classically interpreted as the effect of feldspar (plagioclase) removal during previous fractional crystallization processes. The absence of even the smallest amount of plagioclase in Montefiascone lavas, however, require a different interpretation, inferring the negative Eu/Eu* anomalies as mantle source characteristics. The ultimate origin of these anomalies could be the presence of recycled upper crustal lithologies in Montefiascone lava source, considering the strongly fractionated average composition of average upper crust (e.g., Rudnick and Gao, 2014; Plank, 2014; Gaschning et al., 2016).

The Th/Yb vs. Ta/Yb diagram (Fig. 10) again clearly outlines the influence of subduction-related modifications on all the compositions of all the studied products as well as those of the literature Quaternary volcanic rocks of central Italy. All the analysed and literature whole-rock compositions of Montefiascone are characterized by Th/Nb ratios much higher than those of the oceanic basalts as defined by MORB and OIB, falling in the subduction-modified field.

Isotopic data do confirm this hypothesis, as they undoubtedly indicate the presence of upper crustal components at mantle depths, which indicates derivation from a subduction-modified source. The $^{206}Pb/^{204}Pb$ vs. $^{87}Sr/^{86}Sr$ diagram in Fig. 7c shows a quite good overlap of the Montefiascone samples with the oceanic sediments field. Moreover, the low $^{143}Nd/^{144}Nd$ ratios, ranging between 0.5119 and 0.5126, could be explained invoking a sedimentary input in the source. The whole-rock $\delta^{11}B$ values (from −7.4 to −8.8 ‰) are within the OIB range, but similar and even more negative $\delta^{11}B$ values (down to $\delta^{11}B \sim -20$‰) can also be found in terrigenous sediments (e.g. Agostini et al., 2021 and references therein). Hence, when considering together B and radiogenic isotope ratios, these values could be interpreted as a clue of sediments recycling into the mantle sources of Montefiascone. The boron isotopic

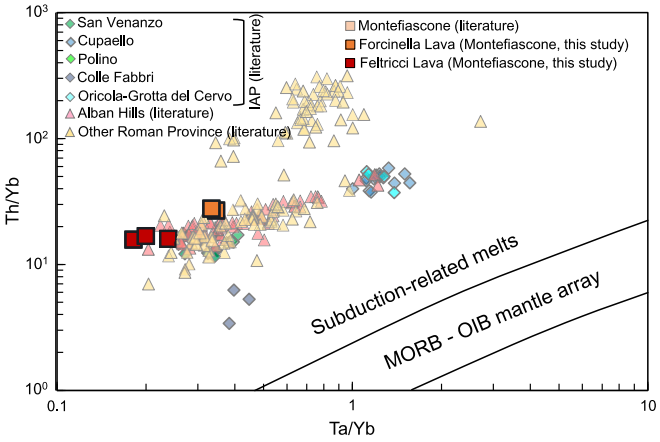

Fig. 10. Th/Yb vs. Ta/Yb diagram (modified after Pearce, 1982). Lava samples from this study are plotted together with Roman Province and IAP literature data. References are reported in Supplementary Material 1.

values for whole rocks reported here are on average less ^{11}B-depleted than the in-situ analyses on melt inclusions from central Italy Quaternary volcanics (Luciani et al., 2023). After remarking that no whole-rock analyses of other volcanic rocks worldwide never exceed −15‰ (e.g., Agostini et al., 2008; Agostini et al., 2021; Marschall, 2018; Tonarini et al., 2005), the high variation range found among the in-situ melt inclusions of Roman Province lavas (e.g., δ^{11}B from −7.4 to −18.3 ‰) may be representative of melt pockets either from primary melts (the highest values), overlapping with the whole-rock data and melt pockets formed later, during and after assimilation of very ^{11}B-depleted sedimentary materials.

5.3. Comparison with other kalsilite-bearing products from central Italy

The Quaternary volcanic provinces of central Italy, the Roman Province and the IAP, are well known in literature as they host also exotic lithologies. IAP includes products with a very variable chemical compositions, including ultrabasic/basic, ultracalcic and ultrapotassic terms (e.g., Gallo et al., 1984; Lustrino et al., 2020), closely resembling Montefiascone compositions from this study. IAP kamafugites are commonly associated to carbonate-rich (CaO up to 39.7 wt%) and silica-poor (SiO_2 down to 14.2 wt%) rocks, whose origin still represents a debated topic, having interpreted either as carbonatites (Stoppa and Cundari, 1996; Stoppa and Woolley, 1997) or as the result of sedimentary limestone assimilation (Lustrino et al., 2019, 2020, 2022b; Peccerillo, 1998, 2017). Due to the large geochemical variations of IAP products, we will refer only to San Venanzo and Cupaello kamafugite lavas (i.e., kamafugite).

The Montefiascone lavas analysed in this study and IAP kamafugites share similar mineral paragenesis and several mineral chemical features (e.g., insufficient Si to fill the T site in clinopyroxene and phlogopite as well as Ca excess in clinopyroxene and olivine). Montefiascone products span from olivine-rich to olivine-free terms. The latter are usually also melilite- and kalsilite-rich. This variability resembles what observed at San Venanzo, where the massive lavas show the same mineralogy but completely different mineral ratios than the San Venanzo pegmatoid facies (Lustrino et al., 2020). Below, we test the possibility to explain the Forcinella and Feltricci kalsilite-bearing rocks as being the products of a prolonged fractional crystallization process involving a parental magma with the composition similar to the most primitive kamafugite rock of San Venanzo reported by Lustrino et al. (2020).

A mass balance model calculated using the MS Excel solver routine is reported in the Supplementary material 3. Sample SAV12 (olivine-phyric melilitite, with clinopyroxene present only in the groundmass) from San Venanzo suite (Lustrino et al., 2020) has been used to represent the parental magma for Forcinella sample MFF6 and Feltricci sample MF4. A good result has been achieved for both the targets, obtaining the sum of the square of the residuals ($\sum R^2$) = 0.01 and being the calculated fractionation coherent either with petrographic and geochemical evidence, either for the Montefiascone and San Venanzo samples (Supplementary material 1). For sample MFF6 the model shows that the crystallization of 31.8% melilite, 19.8% leucite, 18.4% olivine, 5% kalsilite, plus 2.6% Ti-magnetite and 0.8% apatite could actually change the composition of a hypothetical parental magma with the composition of San Venanzo SAV12 sample to a magma represented by Forcinella sample MFF6. A similar result, involving the fractional crystallization of 33.1% melilite, 17.8% leucite, 17.1% olivine, 8.9% kalsilite, 2.9% Ti-magnetite and 0.8% apatite can explain the whole-rock difference between SAV12 and Feltricci sample MF4. Feltricci lava would probably locally hosts cumulus olivine, explaining both the lower amount of crystalizing olivine in the mass balance and the slightly higher MgO of the whole-rock samples.

These results can be interpreted as further evidence of the strict petrogenetic link between these two provinces. Indeed, Montefiascone magmas must be considered as consanguineous of the IAP melts, probably highlighting a similar mantle source paragenesis, but with a prolonged fractionation history.

Additionally, the mass balance calculated for Forcinella sample MFF6 has been further tested for trace-element variation using the Rayleigh fractionation equation (Supplementary material 3). Using the percentage of fractionating phases obtained from the major oxides mass balance and K_D values for literature (see references in the Supplementary material 3), a quite good overlap between the target and the calculated derivative compositions has been observed, with only some elements (e.g., Zr—Hf and HREE) being displaced to higher values in the calculate derivative melt than in the natural Montefiascone sample. By adding to the fractionating assemblage very low amounts (~0.2%) of accessory phases, such as zircon and perovskite, whose presence is reported in literature in San Venanzo lavas (Günther et al., 2023; Lustrino et al., 2020), the few trace element discrepancies disappear (Fig. 11), without causing any relevant variation in the major element budget.

The carbonate plagues in the groundmass of Montefiascone samples, with abundant intergranular melilite and kalsilite, recall the pegmatoid melilitolite facies occurring within the Selvarelle lava flow in San Venanzo. The latter has been interpreted as the product of a more extensive fractionation (74.2 wt%), from the primitive kamafugite melt, of a cumulate constituted by melilite + leucite + olivine + kalsilite + chromite (Lustrino et al., 2020).

The result of fractionation modelling could also help clarifying the hypothesis of crustal assimilation in the Montefiascone Volcanic Complex. The hypothesis of a prolonged crystallization supported by the mass balance makes the carbonate assimilation, during magma ascent and fractionation unlikely. The isotopic compositions of a limestone from the central Apennine (Maiolica limestone formation, Tithonian-Barremian; Barberio et al., 2021) and a marl of an early Miocene pre-flysch deposit have been plotted in the Harker diagrams reported in Fig. 7 and in the Supplementary material 1, together with the lava samples. The two hypothetical contaminants fall, in most cases, in fields far away from the trends generated by the distribution of the samples. This feature, coupled with the isotopic similarities of the Montefiascone lavas with those of San Venanzo igneous rocks seems to confirm a closed-system evolution.

On the other hand, it must be considered that for San Venanzo crustal carbonate assimilation has been proposed (Lustrino et al., 2020) at the beginning of the fractionation, as resulting from many petrographic evidences, such as kirschsteinite rims around olivine, not observed in this study. For Montefiascone, we may conclude that no carbonate

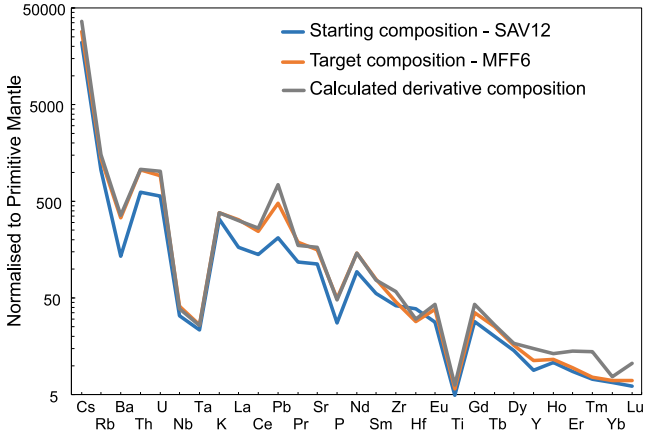

Fig. 11. Primitive mantle-normalised trace element diagram (normalization values after Lyubetskaya and Korenaga, 2007) showing the results of the Rayleigh fractionation model (trace-elements) assuming the San Venanzo primitive sample (SAV12) as starting composition and an evolved lava sample from Montefiascone Volcanic Complex (MFF6) as target melt, using the fractionating mineral assemblage calculated by mass balance and Kd values reported in Supplementary material 3. K, P and Ti values of the calculated derivative melt are taken from major element mass balance calculation.

assimilation is required during the crystallization of the melt, but it could have happened at the beginning of magma ascent to the surface. Further investigations are needed to definitively exclude any relevant involvement of shallow crustal assimilation in the Montefiascone Volcanic Complex evolution.

6. Conclusions

A detailed petrographic, mineral chemical, geochemical and isotopic study has highlighted the presence of rare kalsilite- and melilite-bearing lavas in the Montefiascone Volcanic Complex (Roman Province, central Italy). The studied set of samples coming from two different lava flows, named Forcinella and Feltricci lavas, exhibit different petrographic (e.g., almost total absence of olivine in the Forcinella lava, different modal abundances of melilite and kalsilite) and geochemical features (lower SiO_2 and MgO coupled with higher CaO and K_2O in the Forcinella samples) that may be the result from slightly different fractionation paths from a common kamafugite parental magma, similar to that erupted from the nearby San Venanzo volcano (IAP; Lustrino et al., 2020). A quantitative major oxide and trace element modelling of fractional crystallization strongly corroborates the idea that the differences between the two lava flows depends on a variable evolution and not derivation from on a laterally heterogenous mantle source.

The major and trace elements budgets, as well as Sr, Nd and Pb isotope ratios of the Forcinella and Feltricci lavas match the wider field of the other kalsilite-bearing rocks from central Italy, whereas they strongly differ from those from the two other type localities worldwide where kalsilite-bearing lavas has been recorded (Brazil and Uganda).

Therefore, we expect that the mantle sources underling Montefiascone Complex would closely resemble those of IAP. The presence of peculiar mineral phases, such as kalsilite and melilite, together with the low silica and the extreme enrichment in LILE, could be justified invoking a peridotitic mantle source characterized by metasomatic veins (mainly orthopyroxene-poor to orthopyroxene-free and enriched in phlogopite and clinopyroxene). The high K_2O of the melts, coupled with relatively low Na_2O, involves the presence of phlogopite in the metasomes, whereas the high CaO requires a carbonated/clinopyroxene-rich mantle source. Metasomatic events, possibly related to subducted carbonate sediments, could have led to the development of the metasomatic veins that, after melting and interacting with the surrounding mantle, would have generated kamafugite melts.

To sum up, the kamafugite lavas from Montefiascone fit well in the wider Quaternary potassic and ultrapotassic magmatism of central Italy, which has been largely attributed to a fundamental role of different crustal lithologies, either by contamination and refertilization of the lithospheric mantle or by local wall-rock assimilation during magma uprise (such as in Polino and Alban Hills). Such latter case has not been ultimately ascertained and wholly understood for the Montefiascone Volcanic Complex, as the geochemical and isotopic compositions of the studied rocks do not match with a diffuse crustal carbonate assimilation, as it would have caused a strong dilution of incompatible elements, SiO_2 and K_2O, as well as lowering the $^{87}Sr/^{86}Sr$ ratios. The good results of major element mass balance calculations for fractionation crystallization model supports this hypothesis. Nevertheless, minor assimilation, occurred at depth, during the first stage of the melt uprising cannot be entirely excluded.

CRediT authorship contribution statement

Francesca Innocenzi: Data curation, Formal analysis, Visualization, Writing – original draft. **Sara Ronca:** Conceptualization, Formal analysis, Funding acquisition, Supervision, Writing – review & editing. **Samuele Agostini:** Formal analysis, Funding acquisition, Supervision, Writing – review & editing. **Federica Benedetti:** Formal analysis. **Michele Lustrino:** Conceptualization, Funding acquisition, Supervision, Writing – review & editing.

Declaration of competing interest

The authors declare that they have no known competing financial interests or personal relationships that could have appeared to influence the work reported in this paper.

Acknowledgments

The authors would like to dedicate this contribution to the late prof. Giovanni Nappi, an excellent volcanologist and a great person who dedicated all his life to understanding the dynamics of Italian volcanoes. The authors also thank Domenico Mannetta for his help in the thin sections production, Tania Ruspandini and Matteo Paciucci for SEM-EDS analyses and Marcello Serracino for EMP analyses. FI thanks dr. S. Murray for his help at the Macquarie GeoAnalytical Laboratories. FI is grateful to professors Lorenzo Fedele (University of Naples) and Michele Mattioli (University of Urbino) for their help in improving the manuscript. ML thanks IUGS for the generous support. This work was financially supported by IGG-CNR P-CT0049 funding to SA and Sapienza Fondi Ateneo 2021-2022-2023 to ML and Sapienza Fondi Ateneo 2022 to SR.

Appendix A. Supplementary data

Supplementary data to this article can be found online at https://doi.org/10.1016/j.lithos.2024.107704.

References

Acocella, V., Funiciello, R., 2006. Transverse systems along the extensional Tyrrhenian margin of Central Italy and their influence on volcanism. Tect 25. https://doi.org/10.1029/2005TC001845. TC2003.

Acocella, V., Palladino, D.M., Cioni, R., Russo, P., Simei, S., 2012. Caldera structure, amount of collapse and erupted volumes: the case of Bolsena Caldera, Italy. Geol. Soc. Am. Bull. 124, 1562–1576. https://doi.org/10.1130/B30662.1.

Agostini, S., Ryan, J.G., Tonarini, S., Innocenti, F., 2008. Drying and dying of a subducted slab: coupled Li and B isotope variations in Western Anatolia Cenozoic volcanism. Earth Planet. Sci. Lett. 272, 139–147. https://doi.org/10.1016/j.epsl.2008.04.032.

Agostini, S., Di Giuseppe, P., Mannetti, P., Doglioni, C., Conticelli, S., 2021. A heterogeneous subcontinental mantle under the African-Arabian Plate boundary revealed by boron and radiogenic isotopes. Sci. Rep. 11, 11230. https://doi.org/10.1038/s41598-021-90275-7.

Agostini, S., Di Giuseppe, P., Manetti, P., Savaşçın, M.Y., Conticelli, S., 2022. Geochemical and isotopic (Sr-Nd-Pb) signature of crustal contamination in Na-alkali basaltic magmas of South-East Turkey. Ital. J. Geosci. 141, 363–384. https://doi.org/10.3301/IJG.2022.21.

Ammannati, E., Jacob, D.E., Avanzinelli, R., Foley, S.F., Conticelli, S., 2016. Low Ni olivine in silica-undersaturated ultrapotassic igneous rocks as evidence for carbonate metasomatism in the mantle. Earth Planet. Sci. Lett. 444, 64–74. https://doi.org/10.1016/j.epsl.2016.03.03.

Barberio, M.D., Gori, F., Barbieri, M., Boschetti, T., Caracausi, A., Cardello, G.L., Petitta, M., 2021. Understanding the Origin and Mixing of Deep Fluids in Shallow Aquifers and possible Implications for Crustal Deformation Studies: San Vittorino Plain, Central Apennines. Appl. Sci. 11, 1353. https://doi.org/10.3390/app11041353.

Barchi, M., Landuzzi, A., Minelli, G., Pialli, G.P., 2001. Outer Northern Appennines. In: Vai, G.B., Martini, I.P. (Eds.), Anatomy of an Orogen: The Apennnines and Adjacent Mediterranean Basinis. Kluwer Academic Publishers, Dordrecht, pp. 215–254.

Bea, F., Montero, P., Haissen, F., Rjimati, E., Molina, J.F., Scarrow, J.H., 2014. Kalsilite-bearing plutonic rocks: the deep-seated Archean Awsard massif of the Reguibat rise, South Morocco, West African Craton. Earth Sci. Rev. 138, 1–24. https://doi.org/10.1016/j.earscirev.2014.08.00.

Branca, S., Cinquegrani, A., Cioni, R., Conte, A.M., Conticelli, S., De Astis, G., de Vita, S., De Rosa, R., Di Vito, M.A., Donato, P., Forni, F., 2023. The Italian Quaternary volcanism. Alpine Mediterranean Quatern. 36, 221–284.

Brocchini, D., Di Battistini, G., Laurenzi, M.A., Vernia, L., Bargossi, G.M., 2000. New $^{40}Ar/^{39}Ar$ datings on the southeastern sector of the Vulsinian volcanic district (Central Italy). Ital. J. Geosci. 119, 113–120.

Brod, J.A., Barbosa, E.S.R., Junqueira-Brod, T.C., Gaspar, J.C., Diniz-Pinto, H.S., Sgarbi, P.B.A., Petrinovic, I.A., 2005. The Late-cretaceous Goiás Alkaline Province (GAP), Central Brazil. In: Mesozoic to Cenozoic Alkaline Magmatism in the Brazilian Platform. São Paulo, Edusp/Fapesp, pp. 261–340.

Buonasorte, G., Fiordelisi, A., Pandeli, E., Rossi, U., Sollevanti, F., 1987. Stratigraphic correlations and structural setting of the pre-neoautochtonous sedimentary sequences of Northern Latium. Per. Mineral. 56, 111–122.

Cellai, D., Carpenter, M.A., Heaney, P.J., 1992. Phase transitions and microstructures in natural kaliophilite. Eur. J. Mineral. 4, 1209–1220.
Civetta, L., Del Carmine, P., Manetti, P., Peccerillo, A., Poli, G., 1984. Petrology, geochemistry and Sr-isotope characteristics of lavas from the area of Commenda (Mts. Vulsini, Italy). Bull. Volcanol. 47, 581–595. https://doi.org/10.1007/BF01961228.
Coltorti, M., Di Battistini, G., Nappi, G., Renzulli, A., Zeda, O., 1991. Structural setting and magmatic evolution of Montefiascone Volcanic complex, Vulsini District, Central Italy. J. Volcanol. Geotherm. Res. 46, 99–124. https://doi.org/10.1016/0377-0273(91)90078-E.
Conticelli, S., Peccerillo, A., 1992. Petrology and geochemistry of potassic and ultrapotassic volcanism in Central Italy: petrogenesis and inferences on the evolution of the mantle sources. Lithos 28, 221–240. https://doi.org/10.1016/0024-4937(92)90008-M.
Conticelli, S., Francalanci, L., Manetti, P., Peccerillo, A., 1987. Evolution of Latera Volcano, Vulsinian district (Central Italy): stratigraphical and petrological data. Period. Mineral. 56, 175–199.
Conticelli, S., D'Antonio, M., Pinarelli, L., Civetta, L., 2002. Source contamination and mantle heterogeneity in the genesis of Italian potassic and ultrapotassic volcanic rocks: Sr-Nd-Pb isotope data from Roman Province and Southern Tuscany. Mineral. Petrol. 74, 189–222. https://doi.org/10.1007/s007100200004.
Conticelli, S., Laurenzi, M.A., Giordano, G., Mattei, M., Avanzinelli, R., Melluso, L., Tommasini, S., Boari, E., Cifelli, F., Perini, G., Beltrando, M., 2010. Leucite-bearing (kamafugitic/leucititic) and-free lamproitic ultrapotassic rocks and associated shoshonites from Italy: constraints on petrogenesis and geodynamics. J. Virtual Explor. 36, 1–95.
Davis, F.A., Hirschmann, M.M., Humayun, M., 2011. The composition of the incipient partial melt of garnet peridotite at 3 GPa and the origin of OIB. Earth Planet. Sci. Lett. 308, 380–390. https://doi.org/10.1016/j.epsl.2011.06.00.
Deer, W.A., Howie, R.A., Zussman, J., 2013. An Introduction to the Rock-Forming Minerals. The Mineralogical Society, London, p. 498.
Di Battistini, G., Montanini, A., Vernia, L., Bargossi, G.M., Castorina, F., 1998. Petrology and geochemistry of ultrapotassic rocks from the Montefiascone Volcanic complex (Central Italy): magmatic evolution and petrogenesis. Lithos 43, 169–195. https://doi.org/10.1016/S0024-4937(98)00013-9.
Di Battistini, G., Montanini, A., Vernia, L., Venturelli, G., Tonarini, S., 2001. Petrology of melilite-bearing rocks from the Montefiascone Volcanic complex (Roman Magmatic Province): new insights into the ultrapotassic volcanism of Central Italy. Lithos 59, 1–24. https://doi.org/10.1016/S0024-4937(01)00054-8.
Di Filippo, M., Lombardi, S., Nappi, G., Reimer, G.M., Renzulli, A., Toro, B., 1999. Volcano–tectonic structures, gravity and helium in geothermal areas of Tuscany and Latium (Vulsini volcanic district), Italy. Geothermics 28, 377–393. https://doi.org/10.1016/S0375-6505(99)00014-0.
Foley, S.F., Venturelli, G., Green, D.H., Toscani, L., 1987. The ultrapotassic rocks: characteristics, classification, and constraints for petrogenetic models. Earth-Sci. Rev. 24, 81–134.
Franco, E., De Gennaro, M., 1988. Panunzite; a new mineral from Mt. Somma-Vesuvio, Italy. Am. Mineral. 73, 420–421.
Funiciello, R., de Rita, D., Sposato, A., Esposito, A., Fabbri, M., Marsili, P., Mazzini, I., Paccara, P., Trigari, A., Capelli, G., Faccenna, C., Fiorentino, A., Mazza, R., Rossetti, F., Sardella, R., Soligo, M., Tuccimei, P., Villa, I.M., 2012. Note Illustrative della Carta Geologica d'Italia alla scala 1:50.000, Foglio 354 "Tarquinia". In: Presidenza del Consiglio dei Ministri, Agenzia per la Protezione dell'Ambiente e per i servizi Tecnici: Roma, Italy, Servizio Geologico d'Italia, scale 1:50. 000.
Gallo, F., Giammetti, F., Venturelli, G., Vernia, L., 1984. The kamafugitic rocks of S. Venanzo and Cupaello, Central Italy. Neues Jahrb. Mineral. Monatshefte 5, 198–210.
Gaschning, R.M., Rudnick, R.L., McDonough, W.F., Kaufman, A.J., Valley, J.W., Hu, Z., Gao, S., Beck, M.L., 2016. Compositional evolution of the upper continental crust through time, as constrained by ancient glacial diamictites. Geochim. Cosmochim. Acta 186, 316–343. https://doi.org/10.1016/j.gca.2016.03.020.
Günther, J., Prelević, D., Mertz, D.F., Rocholl, A., Mertz-Kraus, R., Conticelli, S., 2023. Subduction-Legacy and Olivine monitoring for Mantle-Heterogeneities of the sources of Ultrapotassic Magmas: the Italian Case Study. Geochem. Geophys. Geosyst. 24 https://doi.org/10.1029/2022GC010709 e2022GC010709.
Holmes, A., 1950. Petrogenesis of katungite and its associates. Am. Mineral. 35, 772–792.
Innocenzi, F., 2024. Origin of 'Ultra'-Rocks. PhD thesis. University of Rome La Sapienza, Italy, p. 574.
Innocenzi, F., Ronca, S., Agostini, S., Brandano, M., Caracausi, A., Lustrino, M., 2021. The pyroclastic breccias from Cabezo Negro de Tallante (SE Spain): is there any relation with carbonatitic magmatism? Lithos 392, 106140. https://doi.org/10.1016/j.lithos.2021.106140.
Innocenzi, F., Agostini, S., Foley, S., Ronca, S., Lustrino, M., 2023. Kamafugites and kamafugites: a comparison among the Ugandan, Brazilian and Italian variants. In: Goldschmidt Conference Abstract, 16259. https://doi.org/10.7185/gold2023.16259.
Innocenzi, F., Ronca, S., Foley, S.F., Agostini, S., Lustrino, M., 2024. Carbonatitic and ultrabasic magmatism at Toro Ankole and Virunga, western branch of the East African Rift system. Gondwana Res. 125, 317–342. https://doi.org/10.1016/j.gr.2023.09.005.
King, A.J., Phillips, K.J.H., Strekopytov, S., Vita-Finzi, C., Russell, S.S., 2020. Terrestrial modification of the Ivuna meteorite and a reassessment of the chemical composition of the CI type specimen. Geochim. Cosmochim. Acta 268, 73–89. https://doi.org/10.1016/j.gca.2019.09.041.
Le Maitre, R.W., 2002. Classification of Igneous Rocks and Glossary of Terms. Cambridge University Press, Recommendations of the IUGS subcommission on the systematics of igneous rocks, p. 256.
Luciani, N., Nikogosian, I.K., De Hoog, C.J., Davies, G.R., Koornneef, J.M., 2023. Constraints on crustal recycling from boron isotopes in Italian melt inclusions. Earth Planet. Sci. Lett. 624, 118462 https://doi.org/10.1016/j.epsl.2023.118462.
Lustrino, M., Anderson, D.L., 2015. The mantle isotopic printer: basic mantle plume geochemistry for seismologists and geodynamicists. In: Foulger, G.R., Lustrino, M., King, S.D. (Eds.), The interdisciplinary Earth: A volume in honor of Don L. Anderson, 71. Geological Society of America Special Paper 514 and American Geophysical Union Special Publication, pp. 257–279. https://doi.org/10.1130/2015.2514(16.
Lustrino, M., Luciani, N., Stagno, V., 2019. Fuzzy petrology in the origin of carbonatitic/pseudocarbonatitic Ca-rich ultrabasic magma at Polino (Central Italy). Sci. Rep. 9, 1–14. https://doi.org/10.1038/s41598-019-45471-x.
Lustrino, M., Ronca, S., Caracausi, A., Ventura Bordenca, C., Agostini, S., Faraone, D.B., 2020. Strongly SiO_2-undersaturated, CaO-rich kamafugitic Pleistocene magmatism in Central Italy (San Venanzo volcanic complex) and the role of shallow depth limestone assimilation. Earth Sci. Rev. 208, 103256 https://doi.org/10.1016/j.earscirev.2020.103256.
Lustrino, M., Chiarabba, C., Carminati, E., 2022a. Igneous activity in Central-Southern Italy: Is the subduction paradigm still valid? In: Foulger, G.R., Jurdy, D.M., Stein, C. A., Hamilton, L.C., Howard, K., Stein, S. (Eds.), In the Footsteps of Warren B. Hamilton: New Ideas in Earth Science, 553. Geol. Soc. Am. Spec. Paper, Boulder, Colorado, pp. 1–16. https://doi.org/10.1130/2021.2553(28).
Lustrino, M., Pistocchi, L., Ronca, S., Innocenzi, F., Agostini, S., 2022b. Carbonate assimilation of ultrabasic magma: the Pleistocene Cupaello kamafugitic volcano (Central Italy). In: EGU General Assembly, Vienna, Austria, 23-27 May 2022, EGU22-5673. https://doi.org/10.5194/egusphere-egu22-5673.
Lyubetskaya, T., Korenaga, J., 2007. Chemical composition of Earth's primitive mantle and its variance: 1. Method and results. J. Geophys. Res. Solid Earth 112. https://doi.org/10.1029/2005JB004223.
Marini, A., Nappi, G., 1986. Origin and evolution of the Montefiascone caldera (Vulsini volcanoes). Geol. Italia Centrale. Congr. Naz. 73, 299–302.
Marra, F., Jicha, B., Palladino, D.M., Gaeta, M., Costantini, L., Di Buduo, G.M., 2020. $^{40}Ar/^{39}Ar$ single crystal dates from pyroclastic deposits provide a detailed record of the 590-240 ka eruptive period at the Vulsini Volcanic District (Central Italy). J. Volcanol. Geotherm. Res. 398, 106904 https://doi.org/10.1016/j.jvolgeores.2020.106904.
Marschall, H.R., 2018. Boron Isotopes in the Ocean Floor Realm and the Mantle. In: Marschall, H., Foster, G. (Eds.), Boron Isotopes: The Fifth Element. Springer International Publishing, pp. 189–219.
Melluso, L., Conticelli, S., D'Antonio, M., Mirco, N.P., Saccani, E., 2003. Petrology and mineralogy of wollastonite- and melilite-bearing paralavas from the Central Apennines, Italy. Am. Mineral. 88, 1287–1299. https://doi.org/10.2138/am-2003-8-911.
Melluso, L., Lustrino, M., Ruberti, E., Brotzu, P., De Barros Gomes, C., Morbidelli, L., Morra, V., Svisero, D.P., d'Amelio, F., 2008. Major and trace-element compositions of olivine, perovskite, clinopyroxene, Cr-Fe-Ti oxides, phlogopite and host kamafugites and kimberlites, Alto Paranaiba, Brazil. Can. Mineral. 46, 19–40. https://doi.org/10.3749/canmin.46.1.19.
Mugnaioli, E., Bonaccorsi, E., Lanza, A.E., Elkaim, E., Diez-Gómez, V., Sobrados, I., Gemmi, M., Gregorkiewitz, M., 2020. The structure of kaliophilite $KAlSiO_4$, a long-lasting crystallographic problem. Int. Union Crystallogr. J. 7, 1070–1083. https://doi.org/10.1107/S2052252520012270.
Nappi, G., Renzulli, A., Santi, P., 1991. Evidence of incremental growth in the vulsinian calderas (Central Italy). J. Volcanol. Geotherm. Res. 47, 13–31.
Nappi, G., Renzulli, A., Santi, P., Gillot, Y., 1995. Geological evolution and geochronology of the Vulsini volcanic district (Central Italy): Boll. Soc. Geol. Ital. 114, 599–613.
Nappi, G., Antonelli, F., Coltorti, M., Milani, L., Renzulli, A., Siena, F., 1998. Volcanological and petrological evolution of the eastern Vulsini district, Central Italy. J. Volcanol. Geotherm. Res. 87, 211–232. https://doi.org/10.1016/S0377-0273(98)00093-6.
Nappi, G., Chiocchini, U., Bonomo, R., Madonna, S., Mattioli, M., Ricci, V., Vita, L., 2019. Note illustrative del Foglio 345 Viterbo. Carta Geologica d'Italia 1 (50), 000.
Nicoletti, M., Petrucciani, C., Piro, M., Trigila, R., 1981. Nuove datazioni vulsine per uno schema di evoluzione dell'attività vulcanica: Nota II: Il quadrante sud-occidentale: Period. Mineral 50, 141–169.
Palladino, D.M., Simei, S., 2002. Three types of pyroclastic currents and their deposits: examples from the Vulsini Volcanoes, Italy. J. Volcanol. Geotherm. Res. 116, 97–118. https://doi.org/10.1016/S0377-0273(02)00213-5.
Palladino, D.M., Simei, S., 2005. The Latera volcanic complex (Vulsini, Central Italy): Eruptive activity and caldera evolution. Acta Vulcanol. 17, 75–80.
Palladino, D.M., Simei, S., Sottili, G., Trigila, R., 2010. Integrated approach for the reconstruction of stratigraphy and geology of quaternary volcanic terrains: An application to the Vulsini Volcanoes (Central Italy). In: Groppelli, G., Viereck-Goette, L. (Eds.), Stratigraphy and Geology of Volcanic Areas. Geological Society of America Special Paper, pp. 63–84.
Palladino, D.M., Gaeta, M., Giaccio, B., Sottili, G., 2014. On the anatomy of magma chamber and caldera collapse: the example of trachy-phonolitic explosive eruptions of the Roman Province (Central Italy). J. Volcanol. Geotherm. Res. 281, 12–26. https://doi.org/10.1016/j.jvolgeores.2014.05.020.
Pearce, J., 1982. Trace element characteristics of lavas from the destructive plate boundaries. In: Thorpe, R.S. (Ed.), Andesites. John Wiley and Sons, pp. 525–548.

Peccerillo, A., 1998. Relationships between ultrapotassic and carbonate-rich volcanic rocks in Central Italy: petrogenetic and geodynamic implications. Lithos 43, 267–279. https://doi.org/10.1016/S0024-4937(98)00016-4.

Peccerillo, A., 2017. Cenozoic Volcanism in the Tyrrhenian Sea Region. Springer, New Zealand, p. 399.

Peccerillo, A., Federico, M., Barbieri, M., Brilli, M., Wu, T.W., 2010. Interaction between ultrapotassic magmas and carbonate rocks: evidence from geochemical and isotopic (Sr, Nd, O) compositions of granular lithic clasts from the Alban Hills Volcano, Central Italy. Geochim. Cosmochim. Acta 74, 2999–3022. https://doi.org/10.1016/j.gca.2010.02.021.

Plank, T., 2014. The Chemical Composition of Subducting Sediments. In: Keeling, Ralph F. (Ed.), The Crust, Treatise on Geochemistry. Elsevier, Amsterdam, pp. 607–629. https://doi.org/10.1016/B978-0-08-095975-7.00319-3.

Rogers, N.W., Hawkesworth, C.J., Parker, R.J., Marsh, J.S., 1985. The geochemistry of potassic lavas from Vulsini, Central Italy and implications for mantle enrichment processes beneath the Roman region. Contrib. Mineral. Petrol. 90, 244–257. https://doi.org/10.1007/BF00378265.

Rudnick, R.L., Gao, S., 2014. Composition of the continental crust. In: Keeling, Ralph F. (Ed.), The Crust, Treatise on Geochemistry. Elsevier, Amsterdam, pp. 1–51.

Sahama, T.G., 1962. Perthite-like exsolution in the nepheline-kalsilite system. Nor. Geol. Tidsskr. 43, 168–179.

Sahama, T.G., 1974. Potassium-rich alkali rocks. In: Sørensen, H. (Ed.), The Alkaline Rocks. Wiley, New York.

Sgarbi, P.B.A., Valenca, J.G., 1993. Kalsilite in Brazilian kamafugitic rocks. Min. Mag. 57, 165–171. https://doi.org/10.1180/minmag.1993.057.386.16.

Stoppa, F., Cundari, A., 1996. A new Italian carbonatite occurrence at Cupaello Rieti and its genetic significance. Contrib. Mineral. Petrol. 122, 275–288. https://doi.org/10.1007/s004100050127.

Stoppa, F., Woolley, A.R., 1997. The Italian carbonatites: field occurrence, petrology and regional significance. Mineral. Petrol. 59, 43–67.

Tonarini, S., Agostini, S., Innocenti, F., Manetti, P., 2005. $\delta^{11}B$ as tracer of slab dehydration and mantle evolution in western Anatolia Cenozoic magmatism. Terra Nova 17, 259–264. https://doi.org/10.1111/j.1365-3121.2005.00610.x.

Turbeville, B.N., 1992. $^{40}Ar/^{39}Ar$ ages and stratigraphy of the Latera caldera, Italy. Bull. Volcanol. 55, 110–118. https://doi.org/10.1007/BF00301124.

Varekamp, J.C., Kalamarides, R.I., 1989. Hybridization processes in leucite tephrites from Vulsini, Italy, and the evolution of the Italian potassic suite. J. Geophys. Res. Solid Earth 94, 4603–4618. https://doi.org/10.1029/JB094iB04p04603.

Velásquez Ruiz, F., Cordeiro, P., Reich, M., Motta, J.G., Ribeiro, C.C., Angerer, T., Bernardes, R.B., 2022. The genetic link between kamafugite magmatism and alkaline–carbonatite complexes in the Late Cretaceous Alto Paranaíba Igneous Province, Central Brazil. Intern. Geol. Rev. 65, 2148–2170. https://doi.org/10.1080/00206814.2022.2127127.

Woolley, A.R., Bergman, S.C., Edgar, A.D., Le Bas, M.J., Mitchell, R.H., Rock, N.M., Scott Smith, B.H., 1996. Classification of lamprophyres, lamproites, kimberlites, and the kalsilitic, melilitic, and leucitic rocks. The Can. Min. 34, 175–186.